Minor variants of swine H1N1 influenza viruses with enhanced polymerase activity and HA stability promote airborne transmission in ferrets

Meng Hu[1], Jeremy C. Jones[1], Balaji Banoth[1], Chet Raj Ojha[1], Jeri Carol Crumpton[1], Lisa Kercher[1], Robert G. Webster[1], Richard J. Webby[1, 2], and Charles J. Russell[1, 2]

[1]Department of Infectious Diseases, St. Jude Children's Research Hospital, 262 Danny Thomas Place, Memphis, Tennessee 38105-3678, [2]Department of Microbiology, Immunology & Biochemistry, College of Medicine, The University of Tennessee Health Science Center, Memphis, Tennessee 38163.

Running Title: Polymerase activity and HA stability in influenza transmission

*** Corresponding author at:** Department of Infectious Diseases, MS 330, St. Jude Children's Research Hospital, 262 Danny Thomas Place, Memphis, TN 38105-3678, USA. Phone: 901-595-5648. Fax: 901-595-8559. Email: charles.russell@stjude.org.

Keywords: Influenza A virus / swine viruses / polymerase / viral fusion protein / transmissibility / virus adaptation

ABSTRACT

Understanding how animal influenza A viruses (IAVs) acquire airborne transmissibility in humans and ferrets is needed to prepare for and respond to pandemics. Previously, we showed that hemagglutinin (HA) protein stabilization promotes replication and airborne transmission in ferrets using swine H1N1 gamma strains P4 and G15 (Hu et al. 2020). Here, we show that a combination of enhanced polymerase activity and HA stability is necessary for efficient airborne transmission in ferrets and that minor variants containing both properties are quickly selected. P4 and G15 were found to have decreased polymerase activity and relatively poor HA stability, respectively. Polymerase-enhancing variant PA-S321 was selected in half of P4 isolates that airborne-transmitted in ferrets. HA-stabilizing variant HA1-S210 was selected in all G15-inoculated ferrets and was transmitted. With an efficient polymerase and a stable HA, purified G15-HA1-S210 had earlier and higher peak titers in inoculated ferrets and was recovered at a higher frequency after airborne transmission than P4 and G15. Pandemic risk-assessment studies may benefit from deep sequencing capable of identifying minor variants with human-adapted traits.

35 **Introduction**

36 IAVs circulate in numerous species, and it remains challenging to identify animal-origin
37 IAVs at greatest risk to cause a pandemic in humans. In addition to bats (Tong et al. 2012, Tong
38 et al. 2013, Kandeil et al. 2018), IAVs originate from a reservoir of wild aquatic birds (Webster et
39 al. 1992). From wild birds, avian IAVs can infect and either directly or indirectly become endemic
40 in wild and domestic birds, swine, humans, and other domestic or aquatic mammals (Long et al.
41 2019, Russell et al. 2018). IAVs have eight RNA gene segments that encode for over a dozen
42 proteins including an RNA-dependent RNA polymerase (RdRp) complex (PB1, PB2, and PA) and
43 the surface glycoproteins hemagglutinin (HA) and neuraminidase (NA) (Shi et al. 2014,
44 Schrauwen et al. 2014). Antigenically diverse HA and NA subtypes have been identified and
45 currently number from H1-H18 and N1-N11. H1N1 caused the 1918 Spanish influenza pandemic,
46 circulated in humans until 1957, became endemic in swine, reemerged in humans in 1977, and
47 caused the 2009 pandemic (pH1N1) (Webster et al. 2014, Schrauwen et al. 2014). In 1957, H1N1
48 was supplanted in humans by the H2N2 Asian influenza pandemic. H2N2 was supplanted by the
49 H3N2 Hong Kong influenza pandemic in 1968. H3N2 viruses, along with pH1N1 and influenza
50 B viruses, cause seasonal influenza in humans. H1N1, H1N2, and H3N2 viruses are currently
51 endemic in swine (Webby et al. 2004, Gao et al. 2017, Walia et al. 2019). H1 swine viruses have
52 been divided into six clades: alpha (1A.1), beta (1A.2), gamma (1A.3.3.3), H1pandemic (1A.3.3.2),
53 delta1 (1B.2.2), and delta 2 (1B.2.1) (Anderson et al. 2013, Anderson et al. 2016). Swine gamma
54 and pandemic clades diverged approximately twenty years ago and have caused numerous human
55 infections (Pulit-Penaloza et al. 2019). Currently, H1 gamma clade is endemic in swine and
56 frequently reassorts with human pandemic H1N1 isolates (Ducatez et al. 2011). Preparing for and
57 responding to future human pandemics requires an understanding of viral traits and host markers

58 associated with human adaptation so that high-risk emerging viruses can be identified, and
59 countermeasures taken.

60 IAV adaptations that have been associated with human-to-human transmission include HA
61 receptor-binding specificity, HA stability, polymerase complex efficiency, HA-NA balance, NA
62 stalk length, interferon antagonism, and filamentous virus morphology (Lipsitch et al. 2016, Long
63 et al. 2019). During viral entry, the HA protein binds sialic acid-containing receptors. This triggers
64 virion endocytosis and acidification, which induces irreversible HA structural changes that cause
65 membrane fusion. Human-adapted IAVs contain HA proteins that preferentially bind α-2,6-linked
66 sialic acid (SA) receptors over α-2,3-linked ones, which are preferred by avian IAVs (Russell et
67 al. 2006, Schrauwen et al. 2014, Rajao et al. 2018, Van Hoeven et al. 2009, Peacock et al. 2020,
68 Herfst et al. 2020). In human- and ferret-adapted IAVs, the avidity of the HA protein for cell-
69 surface glycan receptors is balanced with the substrate selectivity and catalytic rate of the NA
70 protein (Lipsitch et al. 2016, Zanin et al. 2015, Baum et al. 1991, Yen et al. 2011, Handel et al.
71 2014). Decreased HA activation pH in the context of H5N1 viruses reduces replication and
72 transmission in avian species but increases nasal replication and is required for airborne
73 transmission in ferrets (Imai et al. 2012, Herfst et al. 2012, Shelton et al. 2013, Zaraket et al. 2013a,
74 Reed et al. 2010, Richard et al. 2017, Russell 2014, 2021). Similarly, HA stabilization occurred
75 during the adaptation of pH1N1 to humans (Maurer-Stroh et al. 2010, Klein et al. 2018). HA
76 stabilization has been shown to be necessary for airborne transmission of pH1N1 and swine H1N1
77 gamma viruses in ferrets, in part by increasing longevity of expelled virions (Russier et al. 2016,
78 Singanayagam et al. 2020, Hu et al. 2020).

79 The polymerases from avian IAVs are relatively inefficient at genome replication in
80 mammalian cells (Manz et al. 2012, Cauldwell et al. 2014) Therefore, they require adaptative
81 mutations in their polymerase complexes to replicate and transmit in mammals (Mehle et al. 2009,

82 Gabriel et al. 2011, Gabriel et al. 2014). Mammalian-adaptive PB2 mutations include T271A,
83 G590S, Q591R, E627K, and D701N (Long et al. 2019). PB2-E627K, the best-characterized
84 mutation, was present in the 1918 H1N1, 1957 H2N2, and 1968 H3N2 pandemic viruses and has
85 been associated with avian H7N9 and H5N1 influenza virus adaptation in humans and other
86 mammalian hosts (Liu et al. 2020, Hatta et al. 2001). The 2009 pH1N1 virus lacked the PB2-
87 E627K mutation but had phenotypically similar mutations PB2-G590S/Q591R, which were
88 located near residue 627. The swine H1N1 gamma viruses in the present study have mammalian-
89 preferred PB2-G590S/Q591R mutations and avian-like PB2-E627 and PB2-D701.

90 Influenza pandemic risk assessment algorithms by the US Centers for Disease Control and
91 Prevention (CDC) and World Health Organization (WHO) explicitly consider HA receptor-
92 binding specificity and indirectly account for other human-adaptive viral traits through airborne
93 transmission studies (CDC. 2019, WHO. 2016). Ferrets are currently considered the gold-standard
94 animal model to study transmission of influenza viruses (Van Hoeven et al. 2009, Belser et al.
95 2020). In a recent study, HA stabilization was shown to promote the replication and transmission
96 of swine H1N1 IAVs in ferrets (Hu et al. 2020). Related isolates A/swine/Illinois/2A-1213-
97 G15/2013 (H1N1) and A/swine/Illinois/2B-0314-P4/2014 (H1N1) had a single HA variation at
98 residue 210 (H3 numbering) located between the receptor-binding domain heads, which resulted
99 in HA activation pH values of 5.8 and 5.5, respectively. The G15 group had 3/3 airborne-
100 transmission events in ferrets after selection of a stabilized variant (HA1-S210, HA activation pH
101 5.5). Despite also having an HA activation pH of 5.5, the P4 group had only 1/3 airborne
102 transmission. The G15 and P4 viruses also contained polymerase gene variations at PB2-648 and
103 PA-271, and P4 had minor variants at PA-321 and PA-386. Therefore, it was hypothesized that P4
104 and G15 differ in polymerase activity in addition to HA stability. Differences in both of these
105 properties were suspected to modulate airborne transmissibility in ferrets. The objective of the

106 present study was to use these viruses to understand the relative contributions of HA stability and
107 polymerase activity in the replication and transmission of swine H1N1 gamma viruses in ferrets.
108

109 **Results**

110 **Impact of HA and polymerase variations on gamma virus replication in MDCK cells.**
111 Whole-genome sequencing analyses showed that five amino acid variations existed between swine
112 H1N1 gamma viruses G15 and P4 (Figure 1A). In the present work, we designated the G15 virus
113 as G15-HA1-mixed, because this virus isolate contained 85% HA1-N210 and 15% HA1-S210
114 (Figure 1A). P4 contained 92% PA-N321, 8% PA-S321, 86% PA-D386, and 14% PA-N386, and
115 we designated this virus isolate as P4-PA-mixed. Aside from the minor variants, G15-HA1-mixed
116 and P4-PA-mixed differed from each other at HA1-210, PA-271, and PB2-648 (Figure 1A). From
117 G15-HA1-mixed, we isolated the majority population (G15-HA1-N210) and the minor variant
118 (G15-HA1-S210). Residue HA1-210 interacts with residues across the trimer interface in the head
119 domain. Therefore, the HA1-S210 variant most likely stabilizes the HA protein by resisting
120 dissociation of the heads relative to HA1-N210 (Hu et al. 2020).

121 After infection in Vero cells, the highest pH at which G15-HA1-mixed and G15-HA1-
122 N210 were triggered to cause syncytium formation (cell-to-cell fusion) was 5.8 (Figure 1B). P4-
123 PA-mixed and G15-HA1-S210 had more stable HA proteins that were activated at pH 5.5 and 5.6,
124 respectively. The pH of virus inactivation was measured by exposing virus aliquots to media of
125 varying pH, neutralizing, and measuring residual infectivity. The pH at the midpoint of
126 inactivation of G15-HA1-mixed and G15-HA1-N210 were 5.75 and 5.8, respectively, while those
127 of P4-PA-mixed and G15-HA1-S210 were 5.6 (Figure 1C). Overall, HA activation pH values were
128 similar to virus inactivation values, G15-HA1-mixed and G15-HA1-N210 had relatively unstable
129 HA proteins, and P4-PA-mixed and G15-HA1-S210 had stabilized HA proteins.

130 Previous reports showed polymerase activity and/or HA stability may affect virus one-step
131 growth (Hu et al. 2016, Hu et al. 2017c, Russier et al. 2020). To explore this, we inoculated viruses
132 into MDCK cells at an MOI of 2 PFU/cell and measured the virus titers of the supernatants after
133 6- and 8-hours post-infection (hpi). Compared to P4-PA-mixed, the three other viruses had higher
134 titers at 6 hpi (Figure 1D). As P4-PA-mixed and G15-HA1-S210 have identical HA proteins,
135 enhanced replication at 6 hpi was mapped to the PA-P271 and PB2-L648 variations. At 8 hpi,
136 G15-HA-N210 had higher titers than the other three viruses. G15-HA1-N210 and G15-HA1-S210
137 were identical except for HA1 residue 210. Therefore, the HA1-N210 variation (HA activation pH
138 5.8) enhanced replication at 8 hpi in MDCK cells compared to HA1-S210 (pH 5.6). Similarly,
139 A/TN/1-560/09 (H1N1) Y17H (pH 6.0) yielded higher titers in MDCK after high-MOI inoculation
140 compared to A/TN/1-560/09 wild-type (pH 5.5) (Russier et al. 2020). Overall, both the HA
141 variation and the polymerase variations were found to modulate the production of infectious virus
142 in MDCK cells at relatively early time points.
143
144 **G15 viruses had higher polymerase activity when compared to P4-PA-mixed**. Virus
145 polymerase activity can be assessed by the accumulation of viral mRNA, cRNA, and vRNA, which
146 are produced in virus transcription and replication (Te Velthuis et al. 2018). To study the impact
147 of the PB2 and PA variations on polymerase activity, we compared G15-HA1-S210 and P4-PA-
148 mixed, which had identical HA genes. The viruses were inoculated into MDCK cells at an MOI
149 of 2 PFU/cell and resulting cell lyses and supernatants were harvested at 4 and 6 hpi. Compared
150 to P4-PA-mixed, G15-HA1-S210 had higher mRNA, cRNA, and vRNA levels at 4 and 6 hpi
151 (Figure 2A-B). G15-HA1-S210 also had higher viral loads in cell supernatants at 6 hpi (Figure
152 2C). Overall, the presence of PA-P271 and PB2-L648 in G15-HA1-S210 was associated with

153 higher polymerase activity, and these two variations were also present in G15-HA1-mixed and
154 G15-HA1-N210.

155 **Infection of donor ferrets inoculated with G15-HA1-S210, P4-PA-mixed and G15-**
156 **HA1-mixed.** While G15-HA1-S210 had relatively efficient polymerase activity and a stabilized
157 HA protein, P4-PA-mixed had decreased polymerase activity and G15-HA1-mixed had a
158 relatively unstable HA protein (Figure 3A). Two groups of three ferrets were directly inoculated
159 with 10^6 PFU of each of these viruses, and naïve contact and airborne ferrets were introduced one
160 day later (Figure 3B). Each group was evaluated in an isolated cubicle and personal protective
161 equipment was changed before moving between cubicles to avoid cross contamination of viruses.
162 For P4-PA-mixed and G15-HA1-mixed, data for the second cubicle was obtained previously (Hu
163 et al. 2020) and combined with the present, repeated experiment (which was designated as cubicle
164 one). This was done to reduce the number of animals used and maximize the use of data, complying
165 with the USDA's policy on appropriate use of ferrets. Each cubicle was set to a temperature of
166 approximately 22 °C and relative humidity 40-60 (Figure 3-figure supplement 1). All ferrets were
167 monitored for body weight and temperature daily, and ferret nasal washes were collected every
168 other day until day 14. Ferret sera were collected on day 21.

169 On day 1, G15-HA1-S210 donor ferrets had an average nasal wash titer of 2.18×10^7
170 $TCID_{50}$/ml, a value more than 10-fold higher than that of P4-PA-mixed (6.88×10^5 $TCID_{50}$/ml, P
171 = 0.0065) and 100-fold higher than G15-HA1-mixed (1.08×10^5 $TCID_{50}$/ml, P =0.0001) (Figure
172 3C and Table 1). G15-HA1-S210 had peak titers on day 1, while G15-HA1-mixed and P4-PA-
173 mixed had mean peak titers on days 3 and 2.7, respectively (Figure 3D). Additionally, the average
174 peak titer of G15-HA1-S210 in donor ferrets (2.18×10^7 $TCID_{50}$/ml) was significantly higher than
175 that of G15-HA1-mixed (1.48×10^6 $TCID_{50}$/ml) (Figure 3E). Overall, G15-HA1-S210, which had

176 a stabilized HA and enhanced polymerase activity, had earlier and higher growth in the nasal
177 cavities of inoculated ferrets.

178 Three of six ferrets inoculated with G15-HA1-S210 had >10% body weight loss for at least
179 two days compared to only one of six ferrets inoculated with P4-PA-mixed and G15-HA1-mixed
180 (P = 0.04 and 0.0055, respectively, Figure 3F). No significant differences in body temperature
181 were observed between the donor ferret groups (Figure 3-figure supplement 2).

182 **Contact and airborne transmission in ferrets.** For all three groups, contact transmission
183 occurred at 100% efficiency (6/6) (Figure 4A and 4C). All three viruses grew to similar average
184 peak titers in contact ferrets (G15-HA1-S210, 6.6 $\log_{10}TCID_{50}$/ml, day 4.67; P4-PA-mixed, 6.8
185 $\log_{10}TCID_{50}$/ml, day 4.67; G15-HA1-mixed, 6.5 $\log_{10}TCID_{50}$/ml day 6. ANOVA summary $P >$
186 0.05). We re-cultured nasal washes individually in MDCK cells and harvested isolates growing to
187 detectable titers. For contact groups, we obtained 18 isolates from the nasal washes for each virus
188 (Figure 4D). There were no significant differences in body weight and temperature among the
189 contact (and airborne) groups (Figure 4-figure supplements 1 and 2).

190 The frequency of airborne transmission was similar for all three groups with P4-PA-mixed,
191 G15-HA1-mixed, and G15-HA1-S210 having overall seroconversion rates of 4/6, 5/6, and 4/6,
192 respectively (Table 1). For P4-PA-mixed and G15-HA1-S210, airborne transmission occurred in
193 cubicle 1 in 3/3 ferrets and in cubicle 2 in 1/3 ferrets (Figure 4C). For G15-HA1-mixed, airborne
194 transmission occurred in cubicles 1 and 2 at frequencies of 2/3 and 3/3, respectively. Recovery of
195 virus from the nasal cavities of airborne ferrets occurred for P4-PA-mixed, G15-HA1-mixed, and
196 G15-HA1-S210 at overall frequencies of 4/6, 2/6, and 4/6 (Figure 4B). Thus, G15-HA1-mixed had
197 a slightly higher seroconversion rate (5/6) that the other groups but a lower airborne virus isolation
198 rate (2/6). One ferret in the G15-HA1-S210 had early nasal virus growth on days 2-6, while all of
199 the other airborne ferrets shed nasal virus between days 8 and 14 (Figure 4B). Again, we re-

200 cultured ferret nasal washes in MDCK cells, and found more isolates growing successfully from
201 the G15-HA1-S210 airborne group than from the airborne ferrets in the other two groups (Figure
202 4D and Table 1).

203 **Minor variants selected during transmission enhanced the HA stability and**
204 **polymerase activity of the mixed-population viruses.** We obtained the whole genomes of viruses
205 from ferret nasal washes by next-generation sequencing. For G15-HA1-mixed, the stabilized HA1-
206 S210 became the dominant species within 1-3 days in donors and was transmitted to contact and
207 airborne ferrets (Figure 5C). The transmitted variant was equivalent to the G15-HA1-S210 virus,
208 which maintained the stabilizing HA1-S210 variation in all donor, contact, and airborne samples
209 (Figure 5A). G15-HA1-S210 also contained a variety of minor variants in the donor, contact, and
210 airborne ferrets (Figure 5A). PB1-E751STOP was the most-abundant variant in this group.
211 However, PB1-E751STOP did not emerge on the initial day in airborne ferret A1, and it emerged
212 with a much lower percentage in ferret A3 in cubicle 1 (Figure 5A). Additionally, we didn't detect
213 this variant in the donor and contact ferrets. Therefore, this variant may not be associated with
214 transmission.

215 P4-PA-mixed resulted in 3/3 airborne transmission events in cubicle 1 and 1/3 in cubicle
216 2. Minor variant PA-S321 represented approximately 8% of the inoculum, and this variant became
217 the dominant species in 2/3 airborne-transmission events in cubicle 1 (Figure 5B, 6A). In cubicle
218 2, PA-N321S was recovered in 1/3 contact ferrets but was not recovered from the single airborne
219 ferret. As PA-N321S has been identified as an important human-adaptive mutation for avian H5
220 influenza A viruses (Miotto et al. 2010, El-Shesheny et al. 2014), increased transmission in cubicle
221 1 versus 2 was most likely due to propagation of the PA-S321 variant. We plaque purified P4-PA-
222 S321 and compared this virus *in vitro* to P4-PA-mixed and G15-HA1-S210. P4-PA-S321 had
223 higher levels of mRNA, cRNA, and vRNA at 4 and 6 hpi in MDCK cells than P4-PA-mixed,

224 elevating polymerase activity to a level similar to G15-HA1-S210 (Figure 6B-C). Compared to
225 P4-PA-mixed, P4-PA-S321 also yielded higher virions released from MDCK cells at 6 hpi (Figure
226 6E). P4-PA-S321 yielded RNA levels and virus titers similar to G15-HA1-S210 (Figure 6B-E).
227 Therefore, PA-S321 increased the polymerase activity to a level similar to that of the G15 isolates,
228 which had the alternative polymerase-enhancing variations PA-P271/PB2-L648.

229 The most prevalent variation in G15-HA1-mixed was HA1-S210, which became the
230 dominant species in every ferret. The G15-HA1-mixed inoculum contained approximately 15%
231 HA1-S210 (Figure 7A). HA1-S210 was present at a level greater than 90% in all donor ferrets
232 within three days and was transmitted to all of the contact and airborne animals (Figure 7A).
233 Therefore, all of the contact and airborne ferrets in all three groups contained the stabilizing HA1-
234 S210 variation, resulting in almost all the recovered samples having HA activation pH values of
235 approximately 5.6 (Figure 7B-D). All airborne-transmitted viruses contained a relatively stable
236 HA protein.

237 In summary, P4-PA-mixed had decreased polymerase activity and its transmission could
238 be enhanced by over representation of the PA-S321 variant, and G14-HA1-mixed had a relatively
239 unstable HA protein and its transmission was enhanced by selection of the HA1-S210 variant. Out
240 of thirteen airborne transmission events in ferrets across all three groups, two airborne-transmitted
241 viruses maintained a phenotype of suboptimal polymerase activity and a stabilized HA while
242 eleven had enhanced polymerase activity and a stabilized HA (Figure 8).

243

244

245 **Discussion**

246 Three viral traits thought to be necessary for human-to-human and ferret-to-ferret
247 transmissibility by influenza A viruses are HA receptor-binding specificity for α-2,6-linked sialic-
248 acid receptors, an HA protein relatively resistant to acid-induced activation/inactivation, and a
249 polymerase complex capable of efficient replication in mammalian cells (Lipsitch et al. 2016, Long
250 et al. 2019). The swine H1N1 gamma viruses studied here have been shown to bind α-2,6-linked
251 receptors with high affinity in addition to having lower-level binding to α-2,3-linked receptors (Hu
252 et al. 2020). P4-PA-mixed had a stabilized HA protein but lacked an efficient polymerase, and
253 G15-HA1-mixed had an efficient polymerase but a relatively unstable HA protein. Both virus
254 isolates contained minority variants at a level of 8-15% abundance that overcame the respective
255 deficiency. These variants were selected in ferrets and accounted for 2/4 of P4-PA-mixed and 5/5
256 of G15-HA1-mixed airborne transmission events. Compared to P4-PA-mixed and G15-HA1-
257 mixed, variant G15-HA1-S210, which contained both a stabilized HA protein and an efficient
258 polymerase, had increased early growth in the nasal cavities of inoculated ferrets and was
259 recovered in greater abundance from the nasal cavities of airborne-exposed ferrets. Overall, the
260 data demonstrated that the combination of HA stability and polymerase efficiency is necessary for
261 efficient airborne transmissibility of swine H1N1 gamma viruses in ferrets and that minor variants
262 containing both traits can be rapidly selected and airborne transmitted when the majority of a virus
263 sample lacks a stabilized HA or an efficient polymerase.

264 Multiple traits are required for IAV airborne transmissibility in ferrets, and it is important
265 to understand if these traits must be acquired in a particular order or if they may evolve in any
266 order. For IAVs already possessing α-2,6 receptor-binding specificity, the present study revealed
267 two evolutionary pathways for the enhancement of ferret airborne transmissibility: (A) from a
268 virus quasispecies that has an efficient polymerase, a minor variant with a stabilized HA protein

269 may be selected, or (B) from a virus quasispecies with a stabilized HA protein, a minor variant
270 with an enhanced polymerase may be selected.

271 With respect to pathway A, several other studies showed that an IAV containing α-2,6
272 receptor-binding specificity and an efficient polymerase but having a relatively unstable HA
273 protein can acquire airborne transmissibility in ferrets by acquiring an HA-stabilizing mutation.
274 Wild-type 2009 pH1N1 has an HA activation pH of 5.5, and a destabilizing HA1-Y17H mutation
275 increased this value to 6.0 (Russier et al. 2016, Russier et al. 2017, Russier et al. 2020). The HA1-
276 Y17H mutant was attenuated in ferrets and did not airborne transmit until acquiring stabilizing
277 HA2-R106K and HA1-H17Y mutations, which decreased the HA activation pH to 5.3 (Russier et
278 al. 2016). Mechanistically, HA stabilization was shown to increase replication in human airway
279 cells (Singanayagam et al. 2019), dampen Type I interferon responses in dendritic cells (Russier
280 et al. 2020), and increase the survivability of infectious virions after respiratory expulsion in ferrets
281 (Singanayagam et al. 2020). In another study, a recombinant virus was generated that contained
282 the HA from A/Vietnam/1203/2004 (H5N1) with two HA mutations that conferred α2,6 receptor-
283 binding specificity, and the other seven genes from A/California/04/2009 (H1N1) with a PB2-
284 E627K mutation that enhanced polymerase activity (Imai et al. 2012). This virus and an adaptive
285 mutant containing an HA1-N158D mutation that deleted a glycosylation on the HA head were
286 incapable of airborne transmissibility in ferrets. Instead, a final mutation needed for the acquisition
287 of airborne transmissibility was HA1-T318I in the stalk, which decreased the HA activation pH to
288 5.3. When HA-stabilizing mutations were introduced into other H5N1 viruses lacking α2,6
289 receptor-binding specificity, virus growth in the nasal cavities of ferrets was enhanced but airborne
290 transmission did not occur (Zaraket et al. 2013b, Zaraket et al. 2013a, Shelton et al. 2013).

291 With respect to pathway B, P4-PA-mixed had a stabilized HA protein and its airborne
292 transmission in several instances was associated with selection of the PA-S321 mutation that

293 enhanced polymerase activity. A/Indonesia/5/2005 (H5N1) acquired airborne transmissibility in
294 ferrets by a combination of mutagenesis and adaptation that enhanced receptor-binding activity
295 (HA-T156A and HA-Q222L or HA-G224S), polymerase activity (PB2-E627K and PB1-H99Y),
296 and HA stability (HA-H103Y) (Herfst et al. 2012, Linster et al. 2014). These mutations arose in
297 similar steps during adaptation, and viruses lacking any of the single mutations HA-T156A, PB2-
298 E627K, PB1-H99Y, or HA-H103Y, or both the HA-Q222L or HA-G224S mutations, were loss-
299 of-function for airborne transmission in ferrets. In the case of reassortant IAVs containing genes
300 from the human 1918 virus and avian H1N1 viruses, the human HA gene enabled efficient contact
301 transmission but did not allow airborne transmission in ferrets (Van Hoeven et al. 2009). Instead,
302 the human 1918 PB2 protein was found to be both necessary and sufficient to enable ferret airborne
303 transmission in the context of a virus that contained the human 1918 HA and NA genes.

304 Quasispecies have been associated with IAV fitness and virulence in various hosts (Lauring
305 et al. 2010, Honce et al. 2020). In this study, minor variants of swine H1N1 viruses with enhanced
306 polymerase activity or HA stability were selected in ferrets and associated with airborne
307 transmissibility. The transmission of minor variants has been previously observed for IAVs in
308 humans (Poon et al. 2016), equines (Hughes et al. 2012), and guinea pigs (Varble et al. 2014). This
309 suggests minor variants, in addition to the majority population of a virus, need to be considered
310 when assessing the risk of IAVs for human pandemic potential. Next-generation sequencing has
311 been used to track the outgrowth of HA-stabilizing variants in ferrets in this study and others (Hu
312 et al. 2020, Singanayagam et al. 2020, Russier et al. 2016, Russier et al. 2017). Deep sequencing
313 of samples from H7N9-infected patients and their surrounding poultry/environment showed
314 acquisition of the polymerase-enhancing PB2-E627K variation in humans (Liu et al. 2020). H3N2
315 and H1N1 growth in mice has been shown to not necessarily proceed through linear accumulation
316 of adaptative mutations (Wasik et al. 2019). Overall, as next-generation sequencing becomes

317 cheaper, faster, and more efficient, real-time monitoring of human-adaptive variations may enable
318 better preparedness for future outbreaks.

319 Numerous studies have been performed to identify and characterize human- and ferret-
320 adaptive mutations in IAVs. Examples include those focusing on the polymerase complex (Soh et
321 al. 2019, Jones et al. 2020, Hu et al. 2017b, Hu et al. 2017c, Lee et al. 2021, Goldhill et al. 2021,
322 Mehle et al. 2009, Cheung et al. 2014, Imai et al. 2020) and the HA protein (Lee et al. 2018,
323 Lakdawala et al. 2015, Murakami et al. 2012, DuBois et al. 2011, Stevens et al. 2006, Byrd-Leotis
324 et al. 2015, Zhong et al. 2014, Russier et al. 2017, Singanayagam et al. 2020, Linster et al. 2019,
325 Zaraket et al. 2013b, Reed et al. 2009) In the present study, we found G15 isolates containing PB2-
326 L648/PA-P271 had higher polymerase activities than P4-PA-mixed, which contained PB2-
327 M648/PA-T271. PB2-L648 was previously shown to increase polymerase activity of an H10N8
328 virus (Xiao et al. 2016). The present study also showed that PA-S321 increased polymerase
329 activity. PA-S321 has previously been identified as an adaptative marker for H5N1 influenza A
330 viruses in humans (Miotto et al. 2010, El-Shesheny et al. 2014, Arai et al. 2020). The HA1-S210
331 mutation was shown to decrease the pH of HA activation and the pH of virus inactivation here and
332 in our previous work (Hu et al. 2020).

333 In summary, a combination of efficient polymerase activity and a stabilized HA were found
334 to enhance airborne transmission of swine H1N1 gamma viruses in ferrets, and these two
335 properties may be acquired in either order. Human infections of seasonal influenza viruses have
336 been far less frequent since the start of the SARS-CoV-2 pandemic, mask mandates, and social
337 distancing. Widespread reemergence of seasonal influenza is expected to occur in the post-SARS-
338 CoV-2-pandemic era. Ultimately, exotic IAVs in other species, especially swine, and the potential
339 for cross-species transmission make it essential to monitor potential pandemic IAV strains and to
340 assess their pandemic risk. Swine H1N1 gamma viruses are one of the most prevalent lineages in

341 swine (Diaz et al. 2017), have caused sporadic human infections in recent years (WHO. 2018,
342 Pulit-Penaloza et al. 2019), and have been shown here to acquire increased transmissibility in
343 ferrets by adaptive HA and polymerase mutations. A recent study has identified a swine Eurasian
344 avian-like influenza virus with pandemic traits (Sun et al. 2020). Surveillance and risk assessment
345 studies are needed for IAV pandemic preparedness in addition to studies investigating the
346 evolutionary pathways by which pandemic potential may arise and genetic and phenotypic traits
347 associated therewith.
348

349 **Materials and Methods**

Key Resources Table				
Reagent type (species) or resource	**Designation**	**Source or reference**	**Identifiers**	**Additional information**
animal (*Mustela putorius furo*)	Fitch ferret	Triple F Farms		male, 5-6 months old
cell line (*Canis lupus familiaris*)	MDCK, Madin-Darby Canine Kidney epithelial	ATCC	ATCC Cat# CCL-34, RRID:CVCL_0422	
cell line (*Chlorocebus sabaeus*)	Vero, African green monkey kidney epithelial	ATCC	ATCC Cat# CCL-81, RRID:CVCL_0059	
software	CLC Genomics Workbench 11.0.1	Qiagen		
software	Prism 7	GraphPad		
Strain, strain background (*Influenza A virus*)	A/swine/Illinois/2A-1213-G15/2013 (H1N1)	Genbank	Segments 1-8: MT649710.1, MT649713.1; MT649708.1; MT649712.1; MT649707.1; MT649714.1; MT649709.1; MT649711.1	A_sw_IL_2A1213G15_13
Strain, strain background (*Influenza A virus*)	A/swine/Illinois/2B-0314-P4/2014 (H1N1)	Genbank	Segments 1-8: MT649744.1; MT649743.1; MT649740.1; MT649745.1; MT649742.1; MT649741.1; MT649739.1; MT649746.1	A_sw_IL_2B0314P4_14

350

351 *Cells and viruses*

352 Madin–Darby canine kidney (MDCK) cells were maintained in minimum essential
353 medium (MEM, Thermo Fisher Scientific). African green monkey kidney (Vero) cells were
354 maintained in Dulbecco's Modified Eagle Medium (DMEM, Life Technologies™). Both culture
355 media were supplemented with 10% HyClone® standard fetal bovine serum (FBS, Life

356 Technologies) and 1% penicillin/streptomycin (P/S, Thermo Fisher Scientific). The cells were
357 grown at 37 °C with 5% CO_2 (Hu et al. 2016, Hu et al. 2017c).

358 A/swine/Illinois/2A-1213-G15/2013 (H1N1) (G15-HA1-mixed) and A/swine/Illinois/2B-
359 0314-P4/2014 (H1N1) (P4-PA-mixed) were originally isolated from nasal swabs from pigs in
360 commercial swine herds in the United States that showed symptoms of influenza-like illness, as
361 described previously (Zanin et al. 2017, Hu et al. 2020). G15-HA1-S210 and G15-HA1-N210 were
362 plaque purified twice from MDCK cells using G15-HA1-mixed. The whole-genome sequences of
363 G15-HA1-S210 and G15-HA1-N210 were verified by next-generation sequencing. All viruses
364 were propagated in MDCK cells with 1 μg/ml tosylsulfonyl phenylalanyl chloromethyl ketone
365 (TPCK)–treated trypsin, as described previously (Hu et al. 2016, Hu et al. 2020).

366 *Syncytium assay*

367 Viruses were inoculated into Vero cells in 24–well plates at a multiplicity (MOI) of 3
368 PFU/cell. After maintaining at 37 °C with 5% CO_2 for 16 hours (h), the infected cells were treated
369 with DMEM supplemented with 5 μg/ml TPCK–treated trypsin for 15 minutes (m) and then pH–
370 adjusted PBS buffers for 15 m. Subsequently, the infected cells were maintained in DMEM
371 supplemented with 5% FBS for 3 h at 37 °C. After that, the infected cells were fixed and stained
372 using a Hema 3™ Fixative and Solutions (Fisher Scientific). Syncytia were recorded using a light
373 microscope. The cutoff values for virus HA activation pH were determined at the treated pH that
374 the stained cells in 24-well plates containing more than two syncytia with at least five nuclei, as
375 described previously (Zaraket et al. 2015, Hu et al. 2020, Russier et al. 2020).

376 *HA inactivation pH assay*

377 Tested viruses were treated with a series of pH-adjusted PBS buffers in a ratio of 1:100 for
378 1 h at 37 °C. The resulting infectious viruses were titrated by $TCID_{50}$ on MDCK cells (Russier et
379 al. 2016, Zaraket et al. 2013a). After obtaining virus titers for treatments, HA inactivation pH

380 values were calculated by using GraphPad Prism version 7 software (Graph-Pad Software, San
381 Diego, CA). The parameter LogEC50 was generated using the model Nonlinear Regression
382 [Equation: log (agonist) vs. response-Variable slope (four parameters)] followed by the least
383 squares fitting method.

384 *Virus growth assay*

385 Tested viruses were inoculated into MDCK cells in 24–well plates at an MOI of 2 PFU/cell.
386 After incubation for 1 h at 37 ºC, the infected cells were washed by PBS twice, and continued to
387 be maintained at 37 ºC with MEM culture media (1 ml/well) supplemented with 1 μg/ml TPCK-
388 treated trypsin. At 6- and 8-hours post-infection (hpi), cell culture supernatant was collected and
389 titrated by $TCID_{50}$ on MDCK cells (Hu et al. 2017a, Russier et al. 2016).

390 *Virus mRNA, cRNA and vRNA quantification*

391 Production of virus RNAs (mRNA, cRNA, and vRNA) during influenza A virus
392 transcription and replication processes were quantified using a two-step real time RT-qPCR,
393 modified from the method described previously (Kawakami et al. 2011, Hu et al. 2017b, Hu et al.
394 2017c). Briefly, viruses were inoculated into confluent MDCK cells in 24–well plates at an MOI
395 of 2. The infected cells were incubated at 37 °C for 1 h, washed by PBS twice, and cultured with
396 MEM supplemented with 1 ug/ml TPCK-treated trypsin (1 ml/well). At 4 and 6 hpi, culture
397 supernatants and infected cells were harvested separately.

398 To quantify virus mRNA, cRNA, and vRNA, total RNAs were extracted from the infected
399 cells using RNeasy Mini Kit (Qiagen). The corresponding cDNAs of mRNA, cRNA, and vRNA
400 were generated by reverse-transcription PCR (RT-PCR) using Transcriptor First Strand cDNA
401 Synthesis Kit (Roche). Primers with specific tags for differentiations of virus mRNA, cRNA, and
402 RNA were used (mRNA-RT-PCR primer:
403 CCAGATCGTTCGAGTCGTTTTTTTTTTTTTTTTTCTCATGTTTCT; cRNA-RT-PCR primer:

404 GCTAGCTTCAGCTAGGCATCAGTAGAAACAAGGGTGTTTTTTCTC; vRNA-RT-PCR
405 primer: GGCCGTCATGGTGGCGAATTGGCCACAGGATTAAGGAATATC)
406 Real-time quantitation PCR were performed to quantify these three RNA levels with specific
407 primers targeting virus HA gene (mRNA-real time-forward primer (FP):
408 CCAGTTCATTGGTACTGGTAGTC, mRNA-real time-reverse primer (RP):
409 CCAGATCGTTCGAGTCGT; cRNA-real time-FP: CCAGTTCATTGGTACTGGTAGTC,
410 cRNA-real time-RP: GCTAGCTTCAGCTAGGCATC; vRNA-real time-FP:
411 GGCCGTCATGGTGGCGAAT, vRNA-real time-RP: ACCGTACCACCCATCTATCA;).
412 Internal control GAPDH mRNA was also reverse-transcribed and quantified using oligo $(dT)_{20}$ as
413 RT-PCR primer and the following as real-time PCR primers (FP:
414 ATTCCACCCATGGCAAATTC, RP: CGCTCCTGGAAGATGGTGAT).
415 To quantify viral copy number released in cell-free supernatant, total RNAs were extracted
416 using QIAamp Viral RNA kits (Qiagen). A two-step quantitative real-time reverse-transcription
417 (RT) PCR was applied to quantify viral copy number. The primers used were listed as the
418 following, RT-PCR-primer: AGCAAAAGCAGG; Real-time-FP (targeting NP gene):
419 CTGCTTGTGTGTATGGGCTT; Real-time-RP (targeting NP gene):
420 TGAGCTGGATTTTCATTTGGT. Plasmid PHW2000-NP (G15-HA1-mixed) was used as a
421 standard for quantitative real-time PCR.
422 *Ferret transmission experiments*
423 Thirty-six male Fitch ferrets (five- to six-month-old, purchased from Triple F Farms, Sayre,
424 PA) were verified to be serologically negative for currently circulating influenza A and B viruses
425 and the tested swine H1N1 gamma influenza viruses by HAI assay. At the same time, these ferrets
426 were identified to be serologically negative for currently circulating SARS-CoV-2 by ELISA. The

427 nasal swabs of these ferrets were verified to be negative before the experiments by performing
428 real-time PCR reactions.

429 The transmission study was performed as described in previous work (Hu et al. 2020).
430 Ferret body weight and temperature were monitored daily until day 14. Ferret nasal washes were
431 collected every other day until day 14. Additionally, all ferrets were euthanized on day 21 to collect
432 whole blood. Ferret sera were examined for seroconversion using HAI assay (Zaraket et al. 2015,
433 Russier et al. 2016, Hu et al. 2020). Animal studies were performed in compliance with St. Jude
434 Children's Research Hospital Animal Care and Use Committee guidelines under protocol 459.

435 *Virus whole-genome sequencing and analyses*

436 Virus whole genomes were obtained by next-generation sequencing (Russier et al. 2017,
437 Zaraket et al. 2015, Hu et al. 2020). Viral RNAs were extracted from ferret nasal wash samples or
438 cell-free supernatants using QIAamp Viral RNA kits (Qiagen). The corresponding cDNAs were
439 achieved by reverse–transcription PCR using SuperScript III First-strand Synthesis System
440 (Thermo Fisher Scientific). DNA library was prepared by PCR amplification using Phusion High-
441 Fidelity PCR Master Mix with HF Buffer (New England BioLabs). The resulting PCR products
442 were purified by QIAquick Gel Extraction Kit (Qiagen) and submitted to St Jude Harwell Center
443 for virus whole-genome sequencing.

444 Sequencing data were analyzed using CLC Genomics Workbench version 11.0.1. SNVs
445 resulting amino-acid variations were reported when the predefined quality scores were met and
446 present in forward and reverse reads at an equal ratio. All variants presented in this study were
447 supported by at least 10 reads with a minimum frequency of 5% (unless otherwise stated). Heat
448 maps and parts of whole were generated by using GraphPad Prism version 7 software (GraphPad
449 Software, San Diego, CA).

450 *Statistical analysis*

451 All data analyses were performed using GraphPad Prism version 7. One-way ANOVA
452 followed by a Tukey's multiple comparisons test or Welch's *t* test were used to determine
453 statistical significances. P value < 0.05 was considered significant.
454

455 **Acknowledgments**

456 We thank Guohua Yang, Ashley Webb, and Melissa Penaflor for help with ferret experiments. We
457 also thank St. Jude Animal Resources Center for help with ferret experiments. We thank the
458 Hartwell Center DNA Sequencing & Genotyping, Hartwell Center Functional Genomics, and the
459 Hartwell Center Genome Sequencing Facility. This work was funded, in part, by the National
460 Institute of Allergy and Infectious Diseases under Centers of Excellence for Influenza Research
461 and Surveillance (CEIRS) contract no. HHSN272201400006C, St. Jude Children's Research
462 Hospital, and the American Lebanese Syrian Associated Charities (ALSAC). The content is solely
463 the responsibility of the authors and does not necessarily represent the official views of the
464 National Institutes of Health.

465

466 **Competing interests:** The authors declare no competing financial interests.

467

468 **Author Contributions**

469 Meng Hu, Conceptualization, Data curation, Formal analysis, Supervision, Investigation,
470 Methodology, Writing-original draft, Project administration, Writing-review and editing; Jeremy
471 C. Jones, Balaji Banoth, Chet Raj Ojha, Jeri Carol Crumpton, Investigation; Lisa Kercher,
472 Supervision, Methodology; Robert G. Webster, Resources, Writing-review and editing; Richard J.
473 Webby, Resources, Methodology, Funding acquisition, Writing-review and editing; Charles J.
474 Russell, Conceptualization, Supervision, Methodology, Funding acquisition, Project
475 administration, Writing-review and editing.

476

477 **References**

478 Anderson, T. K., C. A. Macken, N. S. Lewis, R. H. Scheuermann, K. Van Reeth, I. H. Brown, S.
479 L. Swenson, G. Simon, T. Saito, Y. Berhane, J. Ciacci-Zanella, A. Pereda, C. T. Davis,
480 R. O. Donis, R. J. Webby, and A. L. Vincent. 2016. A Phylogeny-Based Global
481 Nomenclature System and Automated Annotation Tool for H1 Hemagglutinin Genes
482 from Swine Influenza A Viruses. *mSphere* **1**. DOI: 10.1128/mSphere.00275-16, PMID:
483 27981236

484 Anderson, T. K., M. I. Nelson, P. Kitikoon, S. L. Swenson, J. A. Korslund, and A. L. Vincent.
485 2013. Population dynamics of cocirculating swine influenza A viruses in the United
486 States from 2009 to 2012. *Influenza Other Respir Viruses* **7 Suppl 4**:42-51. DOI:
487 10.1111/irv.12193, PMID: 24224819

488 Arai, Y., N. Kawashita, E. M. Elgendy, M. S. Ibrahim, T. Daidoji, T. Ono, T. Takagi, T. Nakaya,
489 K. Matsumoto, and Y. Watanabe. 2020. PA Mutations Inherited during Viral Evolution
490 Act Cooperatively To Increase Replication of Contemporary H5N1 Influenza Virus with
491 an Expanded Host Range. *J Virol* **95**. DOI: 10.1128/JVI.01582-20, PMID: 33028722

492 Baum, L. G., and J. C. Paulson. 1991. The N2 neuraminidase of human influenza virus has
493 acquired a substrate specificity complementary to the hemagglutinin receptor specificity.
494 *Virology* **180**:10-5. DOI: 10.1016/0042-6822(91)90003-t, PMID: 1984642

495 Belser, J. A., A. M. Eckert, T. Huynh, J. M. Gary, J. M. Ritter, T. M. Tumpey, and T. R. Maines.
496 2020. A Guide for the Use of the Ferret Model for Influenza Virus Infection. *Am J Pathol*
497 **190**:11-24. DOI: 10.1016/j.ajpath.2019.09.017, PMID: 31654637

498 Byrd-Leotis, L., S. E. Galloway, E. Agbogu, and D. A. Steinhauer. 2015. Influenza
499 hemagglutinin (HA) stem region mutations that stabilize or destabilize the structure of

500 multiple HA subtypes. *J Virol* **89**:4504-16. DOI: 10.1128/JVI.00057-15, PMID:
501 25653452
502 Cauldwell, A. V., J. S. Long, O. Moncorge, and W. S. Barclay. 2014. Viral determinants of
503 influenza A virus host range. *J Gen Virol* **95**:1193-1210. DOI: 10.1099/vir.0.062836-0,
504 PMID: 24584475
505 CDC. 2019. Influenza Risk Assessment Tool (IRAT). Available at:
506 https://www.cdc.gov/flu/pandemic-resources/national-strategy/risk-assessment.htm.
507 Cheung, P. P., S. J. Watson, K. T. Choy, S. Fun Sia, D. D. Wong, L. L. Poon, P. Kellam, Y.
508 Guan, J. S. Malik Peiris, and H. L. Yen. 2014. Generation and characterization of
509 influenza A viruses with altered polymerase fidelity. *Nat Commun* **5**:4794. DOI:
510 10.1038/ncomms5794, PMID: 25183443
511 Diaz, A., D. Marthaler, C. Corzo, C. Munoz-Zanzi, S. Sreevatsan, M. Culhane, and M.
512 Torremorell. 2017. Multiple Genome Constellations of Similar and Distinct Influenza A
513 Viruses Co-Circulate in Pigs During Epidemic Events. *Sci Rep* **7**:11886. DOI:
514 10.1038/s41598-017-11272-3, PMID: 28928365
515 DuBois, R. M., H. Zaraket, M. Reddivari, R. J. Heath, S. W. White, and C. J. Russell. 2011. Acid
516 stability of the hemagglutinin protein regulates H5N1 influenza virus pathogenicity.
517 *PLoS Pathog* **7**:e1002398. DOI: 10.1371/journal.ppat.1002398, PMID: 22144894
518 Ducatez, M. F., B. Hause, E. Stigger-Rosser, D. Darnell, C. Corzo, K. Juleen, R. Simonson, C.
519 Brockwell-Staats, A. Rubrum, D. Wang, A. Webb, J. C. Crumpton, J. Lowe, M. Gramer,
520 and R. J. Webby. 2011. Multiple reassortment between pandemic (H1N1) 2009 and
521 endemic influenza viruses in pigs, United States. *Emerg Infect Dis* **17**:1624-9. DOI:
522 10.3201/eid1709.110338, PMID: 21892996

523 El-Shesheny, R., A. Kandeil, O. Bagato, A. M. Maatouq, Y. Moatasim, A. Rubrum, M. S. Song,
524 R. J. Webby, M. A. Ali, and G. Kayali. 2014. Molecular characterization of avian
525 influenza H5N1 virus in Egypt and the emergence of a novel endemic subclade. *J Gen*
526 *Virol* **95**:1444-1463. DOI: 10.1099/vir.0.063495-0, PMID: 24722680
527 Gabriel, G., and E. Fodor. 2014. Molecular determinants of pathogenicity in the polymerase
528 complex. *Curr Top Microbiol Immunol* **385**:35-60. DOI: 10.1007/82_2014_386, PMID:
529 25033751
530 Gabriel, G., K. Klingel, A. Otte, S. Thiele, B. Hudjetz, G. Arman-Kalcek, M. Sauter, T. Shmidt,
531 F. Rother, S. Baumgarte, B. Keiner, E. Hartmann, M. Bader, G. G. Brownlee, E. Fodor,
532 and H. D. Klenk. 2011. Differential use of importin-alpha isoforms governs cell tropism
533 and host adaptation of influenza virus. *Nat Commun* **2**:156. DOI: 10.1038/ncomms1158,
534 PMID: 21245837
535 Gao, S., T. K. Anderson, R. R. Walia, K. S. Dorman, A. Janas-Martindale, and A. L. Vincent.
536 2017. The genomic evolution of H1 influenza A viruses from swine detected in the
537 United States between 2009 and 2016. *J Gen Virol* **98**:2001-2010. DOI:
538 10.1099/jgv.0.000885, PMID: 28758634
539 Goldhill, D. H., A. Yan, R. Frise, J. Zhou, J. Shelley, A. Gallego Cortes, S. Miah, O. Akinbami,
540 M. Galiano, M. Zambon, A. Lackenby, and W. S. Barclay. 2021. Favipiravir-resistant
541 influenza A virus shows potential for transmission. *PLoS Pathog* **17**:e1008937. DOI:
542 10.1371/journal.ppat.1008937, PMID: 34061908
543 Handel, A., V. Akin, S. S. Pilyugin, V. Zarnitsyna, and R. Antia. 2014. How sticky should a
544 virus be? The impact of virus binding and release on transmission fitness using influenza
545 as an example. *J R Soc Interface* **11**:20131083. DOI: 10.1098/rsif.2013.1083, PMID:
546 24430126

547 Hatta, M., P. Gao, P. Halfmann, and Y. Kawaoka. 2001. Molecular basis for high virulence of
548 Hong Kong H5N1 influenza A viruses. *Science* **293**:1840-2. DOI:
549 10.1126/science.1062882, PMID: 11546875
550 Herfst, S., E. J. Schrauwen, M. Linster, S. Chutinimitkul, E. de Wit, V. J. Munster, E. M. Sorrell,
551 T. M. Bestebroer, D. F. Burke, D. J. Smith, G. F. Rimmelzwaan, A. D. Osterhaus, and R.
552 A. Fouchier. 2012. Airborne transmission of influenza A/H5N1 virus between ferrets.
553 *Science* **336**:1534-41. DOI: 10.1126/science.1213362, PMID: 22723413
554 Herfst, S., J. Zhang, M. Richard, R. McBride, P. Lexmond, T. M. Bestebroer, M. I. J. Spronken,
555 D. de Meulder, J. M. van den Brand, M. E. Rosu, S. R. Martin, S. J. Gamblin, X. Xiong,
556 W. Peng, R. Bodewes, E. van der Vries, Adme Osterhaus, J. C. Paulson, J. J. Skehel, and
557 R. A. M. Fouchier. 2020. Hemagglutinin Traits Determine Transmission of Avian
558 A/H10N7 Influenza Virus between Mammals. *Cell Host Microbe* **28**:602-613 e7. DOI:
559 10.1016/j.chom.2020.08.011, PMID: 33031770
560 Honce, R., E. A. Karlsson, N. Wohlgemuth, L. D. Estrada, V. A. Meliopoulos, J. Yao, and S.
561 Schultz-Cherry. 2020. Obesity-Related Microenvironment Promotes Emergence of
562 Virulent Influenza Virus Strains. *mBio* **11**. DOI: 10.1128/mBio.03341-19, PMID:
563 32127459
564 Hu, M., H. Chu, K. Zhang, K. Singh, C. Li, S. Yuan, B. K. Chow, W. Song, J. Zhou, and B. J.
565 Zheng. 2016. Amino acid substitutions V63I or A37S/I61T/V63I/V100A in the PA N-
566 terminal domain increase the virulence of H7N7 influenza A virus. *Sci Rep* **6**:37800.
567 DOI: 10.1038/srep37800, PMID: 27886255
568 Hu, M., G. Yang, J. DeBeauchamp, J. C. Crumpton, H. Kim, L. Li, X. F. Wan, L. Kercher, A. S.
569 Bowman, R. G. Webster, R. J. Webby, and C. J. Russell. 2020. HA stabilization

570 promotes replication and transmission of swine H1N1 gamma influenza viruses in ferrets.
571 *Elife* **9**. DOI: 10.7554/eLife.56236, PMID: 32602461
572 Hu, M., S. Yuan, Z. W. Ye, K. Singh, C. Li, H. Shuai, N. Fai, B. K. C. Chow, H. Chu, and B. J.
573 Zheng. 2017a. PAN substitutions A37S, A37S/I61T and A37S/V63I attenuate the
574 replication of H7N7 influenza A virus by impairing the polymerase and endonuclease
575 activities. *J Gen Virol* **98**:364-373. DOI: 10.1099/jgv.0.000717, PMID: 28113045
576 Hu, M., S. Yuan, Z. W. Ye, K. Singh, C. Li, H. Shuai, N. Fai, B. K. Chow, H. Chu, and B. J.
577 Zheng. 2017b. PAN substitutions A37S, A37S/I61T and A37S/V63I attenuate the
578 replication of H7N7 influenza A virus by impairing the polymerase and endonuclease
579 activities. *J Gen Virol* **98**:364-373. DOI: 10.1099/jgv.0.000717, PMID: 28113045
580 Hu, M., S. Yuan, K. Zhang, K. Singh, Q. Ma, J. Zhou, H. Chu, and B. J. Zheng. 2017c. PB2
581 substitutions V598T/I increase the virulence of H7N9 influenza A virus in mammals.
582 *Virology* **501**:92-101. DOI: 10.1016/j.virol.2016.11.008, PMID: 27889648
583 Hughes, J., R. C. Allen, M. Baguelin, K. Hampson, G. J. Baillie, D. Elton, J. R. Newton, P.
584 Kellam, J. L. Wood, E. C. Holmes, and P. R. Murcia. 2012. Transmission of equine
585 influenza virus during an outbreak is characterized by frequent mixed infections and
586 loose transmission bottlenecks. *PLoS Pathog* **8**:e1003081. DOI:
587 10.1371/journal.ppat.1003081, PMID: 23308065
588 Imai, M., T. Watanabe, M. Hatta, S. C. Das, M. Ozawa, K. Shinya, G. Zhong, A. Hanson, H.
589 Katsura, S. Watanabe, C. Li, E. Kawakami, S. Yamada, M. Kiso, Y. Suzuki, E. A.
590 Maher, G. Neumann, and Y. Kawaoka. 2012. Experimental adaptation of an influenza H5
591 HA confers respiratory droplet transmission to a reassortant H5 HA/H1N1 virus in
592 ferrets. *Nature* **486**:420-8. DOI: 10.1038/nature10831, PMID: 22722205

593 Imai, M., M. Yamashita, Y. Sakai-Tagawa, K. Iwatsuki-Horimoto, M. Kiso, J. Murakami, A.
594 Yasuhara, K. Takada, M. Ito, N. Nakajima, K. Takahashi, T. J. S. Lopes, J. Dutta, Z.
595 Khan, D. Kriti, H. van Bakel, A. Tokita, H. Hagiwara, N. Izumida, H. Kuroki, T.
596 Nishino, N. Wada, M. Koga, E. Adachi, D. Jubishi, H. Hasegawa, and Y. Kawaoka.
597 2020. Influenza A variants with reduced susceptibility to baloxavir isolated from
598 Japanese patients are fit and transmit through respiratory droplets. *Nat Microbiol* **5**:27-33.
599 DOI: 10.1038/s41564-019-0609-0, PMID: 31768027
600 Jones, J. C., P. N. Q. Pascua, T. P. Fabrizio, B. M. Marathe, P. Seiler, S. Barman, R. J. Webby,
601 R. G. Webster, and E. A. Govorkova. 2020. Influenza A and B viruses with reduced
602 baloxavir susceptibility display attenuated in vitro fitness but retain ferret
603 transmissibility. *Proc Natl Acad Sci U S A* **117**:8593-8601. DOI:
604 10.1073/pnas.1916825117, PMID: 32217734
605 Kandeil, A., M. R. Gomaa, M. M. Shehata, A. N. El Taweel, S. H. Mahmoud, O. Bagato, Y.
606 Moatasim, O. Kutkat, A. S. Kayed, P. Dawson, X. Qiu, J. Bahl, R. J. Webby, W. B.
607 Karesh, G. Kayali, and M. A. Ali. 2018. Isolation and characterization of a distinct
608 influenza A virus from Egyptian bats. *J Virol*. DOI: 10.1128/JVI.01059-18, PMID:
609 30381492
610 Kawakami, E., T. Watanabe, K. Fujii, H. Goto, S. Watanabe, T. Noda, and Y. Kawaoka. 2011.
611 Strand-specific real-time RT-PCR for distinguishing influenza vRNA, cRNA, and
612 mRNA. *J Virol Methods* **173**:1-6. DOI: 10.1016/j.jviromet.2010.12.014, PMID:
613 21185869
614 Klein, E. Y., D. Blumenkrantz, A. Serohijos, E. Shakhnovich, J. M. Choi, J. V. Rodrigues, B. D.
615 Smith, A. P. Lane, A. Feldman, and A. Pekosz. 2018. Stability of the Influenza Virus

616 Hemagglutinin Protein Correlates with Evolutionary Dynamics. *mSphere* **3**. DOI:
617 10.1128/mSphereDirect.00554-17, PMID: 29299534
618 Lakdawala, S. S., A. Jayaraman, R. A. Halpin, E. W. Lamirande, A. R. Shih, T. B. Stockwell, X.
619 Lin, A. Simenauer, C. T. Hanson, L. Vogel, M. Paskel, M. Minai, I. Moore, M. Orandle,
620 S. R. Das, D. E. Wentworth, R. Sasisekharan, and K. Subbarao. 2015. The soft palate is
621 an important site of adaptation for transmissible influenza viruses. *Nature* **526**:122-5.
622 DOI: 10.1038/nature15379, PMID: 26416728
623 Lauring, A. S., and R. Andino. 2010. Quasispecies theory and the behavior of RNA viruses.
624 *PLoS Pathog* **6**:e1001005. DOI: 10.1371/journal.ppat.1001005, PMID: 20661479
625 Lee, J. M., J. Huddleston, M. B. Doud, K. A. Hooper, N. C. Wu, T. Bedford, and J. D. Bloom.
626 2018. Deep mutational scanning of hemagglutinin helps predict evolutionary fates of
627 human H3N2 influenza variants. *Proc Natl Acad Sci U S A* **115**:E8276-E8285. DOI:
628 10.1073/pnas.1806133115, PMID: 30104379
629 Lee, L. Y., J. Zhou, P. Koszalka, R. Frise, R. Farrukee, K. Baba, S. Miah, T. Shishido, M.
630 Galiano, T. Hashimoto, S. Omoto, T. Uehara, E. J. Mifsud, N. Collinson, K. Kuhlbusch,
631 B. Clinch, S. Wildum, W. S. Barclay, and A. C. Hurt. 2021. Evaluating the fitness of
632 PA/I38T-substituted influenza A viruses with reduced baloxavir susceptibility in a
633 competitive mixtures ferret model. *PLoS Pathog* **17**:e1009527. DOI:
634 10.1371/journal.ppat.1009527, PMID: 33956888
635 Linster, M., E. J. A. Schrauwen, S. van der Vliet, D. F. Burke, P. Lexmond, T. M. Bestebroer, D.
636 J. Smith, S. Herfst, B. F. Koel, and R. A. M. Fouchier. 2019. The Molecular Basis for
637 Antigenic Drift of Human A/H2N2 Influenza Viruses. *J Virol* **93**. DOI:
638 10.1128/JVI.01907-18, PMID: 30700609

639 Linster, M., S. van Boheemen, M. de Graaf, E. J. A. Schrauwen, P. Lexmond, B. Manz, T. M.
640 Bestebroer, J. Baumann, D. van Riel, G. F. Rimmelzwaan, Adme Osterhaus, M.
641 Matrosovich, R. A. M. Fouchier, and S. Herfst. 2014. Identification, characterization, and
642 natural selection of mutations driving airborne transmission of A/H5N1 virus. *Cell*
643 **157**:329-339. DOI: 10.1016/j.cell.2014.02.040, PMID: 24725402
644 Lipsitch, M., W. Barclay, R. Raman, C. J. Russell, J. A. Belser, S. Cobey, P. M. Kasson, J. O.
645 Lloyd-Smith, S. Maurer-Stroh, S. Riley, C. A. Beauchemin, T. Bedford, T. C. Friedrich,
646 A. Handel, S. Herfst, P. R. Murcia, B. Roche, C. O. Wilke, and C. A. Russell. 2016. Viral
647 factors in influenza pandemic risk assessment. *Elife* **5**. DOI: 10.7554/eLife.18491, PMID:
648 27834632
649 Liu, W. J., J. Li, R. Zou, J. Pan, T. Jin, L. Li, P. Liu, Y. Zhao, X. Yu, H. Wang, G. Liu, H. Jiang,
650 Y. Bi, L. Liu, K. Y. Yuen, Y. Liu, and G. F. Gao. 2020. Dynamic PB2-E627K
651 substitution of influenza H7N9 virus indicates the in vivo genetic tuning and rapid host
652 adaptation. *Proc Natl Acad Sci U S A* **117**:23807-23814. DOI: 10.1073/pnas.2013267117,
653 PMID: 32873642
654 Long, J. S., B. Mistry, S. M. Haslam, and W. S. Barclay. 2019. Host and viral determinants of
655 influenza A virus species specificity. *Nat Rev Microbiol* **17**:67-81. DOI: 10.1038/s41579-
656 018-0115-z, PMID: 30487536
657 Manz, B., L. Brunotte, P. Reuther, and M. Schwemmle. 2012. Adaptive mutations in NEP
658 compensate for defective H5N1 RNA replication in cultured human cells. *Nat Commun*
659 **3**:802. DOI: 10.1038/ncomms1804, PMID: 22549831
660 Maurer-Stroh, S., R. T. Lee, F. Eisenhaber, L. Cui, S. P. Phuah, and R. T. Lin. 2010. A new
661 common mutation in the hemagglutinin of the 2009 (H1N1) influenza A virus. *PLoS*
662 *Curr* **2**:RRN1162. DOI: 10.1371/currents.rrn1162, PMID: 20535229

663 Mehle, A., and J. A. Doudna. 2009. Adaptive strategies of the influenza virus polymerase for
664 replication in humans. *Proc Natl Acad Sci U S A* **106**:21312-6. DOI:
665 10.1073/pnas.0911915106, PMID: 19995968
666 Miotto, O., A. T. Heiny, R. Albrecht, A. Garcia-Sastre, T. W. Tan, J. T. August, and V. Brusic.
667 2010. Complete-proteome mapping of human influenza A adaptive mutations:
668 implications for human transmissibility of zoonotic strains. *PLoS One* **5**:e9025. DOI:
669 10.1371/journal.pone.0009025, PMID: 20140252
670 Murakami, S., T. Horimoto, M. Ito, R. Takano, H. Katsura, M. Shimojima, and Y. Kawaoka.
671 2012. Enhanced growth of influenza vaccine seed viruses in vero cells mediated by
672 broadening the optimal pH range for virus membrane fusion. *J Virol* **86**:1405-10. DOI:
673 10.1128/JVI.06009-11, PMID: 22090129
674 Peacock, T. P., J. E. Sealy, W. T. Harvey, D. J. Benton, R. Reeve, and M. Iqbal. 2020. Genetic
675 determinants of receptor-binding preference and zoonotic potential of H9N2 avian
676 influenza viruses. *J Virol*. DOI: 10.1128/JVI.01651-20, PMID: 33268517
677 Poon, L. L., T. Song, R. Rosenfeld, X. Lin, M. B. Rogers, B. Zhou, R. Sebra, R. A. Halpin, Y.
678 Guan, A. Twaddle, J. V. DePasse, T. B. Stockwell, D. E. Wentworth, E. C. Holmes, B.
679 Greenbaum, J. S. Peiris, B. J. Cowling, and E. Ghedin. 2016. Quantifying influenza virus
680 diversity and transmission in humans. *Nat Genet* **48**:195-200. DOI: 10.1038/ng.3479,
681 PMID: 26727660
682 Pulit-Penaloza, J. A., J. A. Belser, T. M. Tumpey, and T. R. Maines. 2019. Sowing the Seeds of a
683 Pandemic? Mammalian Pathogenicity and Transmissibility of H1 Variant Influenza
684 Viruses from the Swine Reservoir. *Trop Med Infect Dis* **4**. DOI:
685 10.3390/tropicalmed4010041, PMID: 30818793

686 Rajao, D. S., T. K. Anderson, P. Kitikoon, J. Stratton, N. S. Lewis, and A. L. Vincent. 2018.
687 Antigenic and genetic evolution of contemporary swine H1 influenza viruses in the
688 United States. *Virology* **518**:45-54. DOI: 10.1016/j.virol.2018.02.006, PMID: 29453058
689 Reed, M. L., O. A. Bridges, P. Seiler, J. K. Kim, H. L. Yen, R. Salomon, E. A. Govorkova, R. G.
690 Webster, and C. J. Russell. 2010. The pH of activation of the hemagglutinin protein
691 regulates H5N1 influenza virus pathogenicity and transmissibility in ducks. *J Virol*
692 **84**:1527-35. DOI: 10.1128/JVI.02069-09, PMID: 19923184
693 Reed, M. L., H. L. Yen, R. M. DuBois, O. A. Bridges, R. Salomon, R. G. Webster, and C. J.
694 Russell. 2009. Amino acid residues in the fusion peptide pocket regulate the pH of
695 activation of the H5N1 influenza virus hemagglutinin protein. *J Virol* **83**:3568-80. DOI:
696 10.1128/JVI.02238-08, PMID: 19193808
697 Richard, M., S. Herfst, J. M. A. van den Brand, D. de Meulder, P. Lexmond, T. M. Bestebroer,
698 and R. A. M. Fouchier. 2017. Mutations Driving Airborne Transmission of A/H5N1
699 Virus in Mammals Cause Substantial Attenuation in Chickens only when combined. *Sci*
700 *Rep* **7**:7187. DOI: 10.1038/s41598-017-07000-6, PMID: 28775271
701 Russell, C. J. 2014. Acid-induced membrane fusion by the hemagglutinin protein and its role in
702 influenza virus biology. *Curr Top Microbiol Immunol* **385**:93-116. DOI:
703 10.1007/82_2014_393, PMID: 25007844
704 Russell, C. J. 2021. Hemagglutinin Stability and Its Impact on Influenza A Virus Infectivity,
705 Pathogenicity, and Transmissibility in Avians, Mice, Swine, Seals, Ferrets, and Humans.
706 *Viruses* **13**. DOI: 10.3390/v13050746, PMID: 33923198
707 Russell, C. J., M. Hu, and F. A. Okda. 2018. Influenza Hemagglutinin Protein Stability,
708 Activation, and Pandemic Risk. *Trends Microbiol*. DOI: 10.1016/j.tim.2018.03.005,
709 PMID: 29681430

710 Russell, R. J., D. J. Stevens, L. F. Haire, S. J. Gamblin, and J. J. Skehel. 2006. Avian and human
711 receptor binding by hemagglutinins of influenza A viruses. *Glycoconj J* **23**:85-92. DOI:
712 10.1007/s10719-006-5440-1, PMID: 16575525
713 Russier, M., G. Yang, B. Briard, V. Meliopoulos, S. Cherry, T. D. Kanneganti, S. Schultz-
714 Cherry, P. Vogel, and C. J. Russell. 2020. Hemagglutinin Stability Regulates H1N1
715 Influenza Virus Replication and Pathogenicity in Mice by Modulating Type I Interferon
716 Responses in Dendritic Cells. *J Virol* **94**. DOI: 10.1128/JVI.01423-19, PMID: 31694942
717 Russier, M., G. Yang, A. Marinova-Petkova, P. Vogel, B. S. Kaplan, R. J. Webby, and C. J.
718 Russell. 2017. H1N1 influenza viruses varying widely in hemagglutinin stability transmit
719 efficiently from swine to swine and to ferrets. *PLoS Pathog* **13**:e1006276. DOI:
720 10.1371/journal.ppat.1006276, PMID: 28282440
721 Russier, M., G. Yang, J. E. Rehg, S. S. Wong, H. H. Mostafa, T. P. Fabrizio, S. Barman, S.
722 Krauss, R. G. Webster, R. J. Webby, and C. J. Russell. 2016. Molecular requirements for
723 a pandemic influenza virus: An acid-stable hemagglutinin protein. *Proc Natl Acad Sci U*
724 *S A* **113**:1636-41. DOI: 10.1073/pnas.1524384113, PMID: 26811446
725 Schrauwen, E. J., and R. A. Fouchier. 2014. Host adaptation and transmission of influenza A
726 viruses in mammals. *Emerg Microbes Infect* **3**:e9. DOI: 10.1038/emi.2014.9, PMID:
727 26038511
728 Shelton, H., K. L. Roberts, E. Molesti, N. Temperton, and W. S. Barclay. 2013. Mutations in
729 haemagglutinin that affect receptor binding and pH stability increase replication of a PR8
730 influenza virus with H5 HA in the upper respiratory tract of ferrets and may contribute to
731 transmissibility. *J Gen Virol* **94**:1220-9. DOI: 10.1099/vir.0.050526-0, PMID: 23486663

732 Shi, Y., Y. Wu, W. Zhang, J. Qi, and G. F. Gao. 2014. Enabling the 'host jump': structural
733 determinants of receptor-binding specificity in influenza A viruses. *Nat Rev Microbiol*
734 **12**:822-31. DOI: 10.1038/nrmicro3362, PMID: 25383601
735 Singanayagam, A., M. Zambon, and W. S. Barclay. 2019. Influenza Virus with Increased pH of
736 Hemagglutinin Activation Has Improved Replication in Cell Culture but at the Cost of
737 Infectivity in Human Airway Epithelium. *J Virol* **93**. DOI: 10.1128/JVI.00058-19, PMID:
738 31189708
739 Singanayagam, A., J. Zhou, R. A. Elderfield, R. Frise, J. Ashcroft, M. Galiano, S. Miah, L.
740 Nicolaou, and W. S. Barclay. 2020. Characterising viable virus from air exhaled by
741 H1N1 influenza-infected ferrets reveals the importance of haemagglutinin stability for
742 airborne infectivity. *PLoS Pathog* **16**:e1008362. DOI: 10.1371/journal.ppat.1008362,
743 PMID: 32097448
744 Soh, Y. S., L. H. Moncla, R. Eguia, T. Bedford, and J. D. Bloom. 2019. Comprehensive mapping
745 of adaptation of the avian influenza polymerase protein PB2 to humans. *Elife* **8**. DOI:
746 10.7554/eLife.45079, PMID: 31038123
747 Stevens, J., O. Blixt, T. M. Tumpey, J. K. Taubenberger, J. C. Paulson, and I. A. Wilson. 2006.
748 Structure and receptor specificity of the hemagglutinin from an H5N1 influenza virus.
749 *Science* **312**:404-10. DOI: 10.1126/science.1124513, PMID: 16543414
750 Sun, H., Y. Xiao, J. Liu, D. Wang, F. Li, C. Wang, C. Li, J. Zhu, J. Song, H. Sun, Z. Jiang, L.
751 Liu, X. Zhang, K. Wei, D. Hou, J. Pu, Y. Sun, Q. Tong, Y. Bi, K. C. Chang, S. Liu, G. F.
752 Gao, and J. Liu. 2020. Prevalent Eurasian avian-like H1N1 swine influenza virus with
753 2009 pandemic viral genes facilitating human infection. *Proc Natl Acad Sci U S A*
754 **117**:17204-17210. DOI: 10.1073/pnas.1921186117, PMID: 32601207

755 Te Velthuis, A. J. W., J. S. Long, and W. S. Barclay. 2018. Assays to Measure the Activity of
756 Influenza Virus Polymerase. *Methods Mol Biol* **1836**:343-374. DOI: 10.1007/978-1-
757 4939-8678-1_17, PMID: 30151582
758 Tong, S., Y. Li, P. Rivailler, C. Conrardy, D. A. Castillo, L. M. Chen, S. Recuenco, J. A. Ellison,
759 C. T. Davis, I. A. York, A. S. Turmelle, D. Moran, S. Rogers, M. Shi, Y. Tao, M. R.
760 Weil, K. Tang, L. A. Rowe, S. Sammons, X. Xu, M. Frace, K. A. Lindblade, N. J. Cox,
761 L. J. Anderson, C. E. Rupprecht, and R. O. Donis. 2012. A distinct lineage of influenza A
762 virus from bats. *Proc Natl Acad Sci U S A* **109**:4269-74. DOI: 10.1073/pnas.1116200109,
763 PMID: 22371588
764 Tong, S., X. Zhu, Y. Li, M. Shi, J. Zhang, M. Bourgeois, H. Yang, X. Chen, S. Recuenco, J.
765 Gomez, L. M. Chen, A. Johnson, Y. Tao, C. Dreyfus, W. Yu, R. McBride, P. J. Carney,
766 A. T. Gilbert, J. Chang, Z. Guo, C. T. Davis, J. C. Paulson, J. Stevens, C. E. Rupprecht,
767 E. C. Holmes, I. A. Wilson, and R. O. Donis. 2013. New world bats harbor diverse
768 influenza A viruses. *PLoS Pathog* **9**:e1003657. DOI: 10.1371/journal.ppat.1003657,
769 PMID: 24130481
770 Van Hoeven, N., C. Pappas, J. A. Belser, T. R. Maines, H. Zeng, A. Garcia-Sastre, R.
771 Sasisekharan, J. M. Katz, and T. M. Tumpey. 2009. Human HA and polymerase subunit
772 PB2 proteins confer transmission of an avian influenza virus through the air. *Proc Natl*
773 *Acad Sci U S A* **106**:3366-71. DOI: 10.1073/pnas.0813172106, PMID: 19211790
774 Varble, A., R. A. Albrecht, S. Backes, M. Crumiller, N. M. Bouvier, D. Sachs, A. Garcia-Sastre,
775 and B. R. tenOever. 2014. Influenza A virus transmission bottlenecks are defined by
776 infection route and recipient host. *Cell Host Microbe* **16**:691-700. DOI:
777 10.1016/j.chom.2014.09.020, PMID: 25456074

778 Walia, R. R., T. K. Anderson, and A. L. Vincent. 2019. Regional patterns of genetic diversity in
779 swine influenza A viruses in the United States from 2010 to 2016. *Influenza Other Respir*
780 *Viruses* **13**:262-273. DOI: 10.1111/irv.12559, PMID: 29624873
781 Wasik, B. R., I. E. H. Voorhees, K. N. Barnard, B. K. Alford-Lawrence, W. S. Weichert, G.
782 Hood, A. Nogales, L. Martinez-Sobrido, E. C. Holmes, and C. R. Parrish. 2019. Influenza
783 Viruses in Mice: Deep Sequencing Analysis of Serial Passage and Effects of Sialic Acid
784 Structural Variation. *J Virol* **93**. DOI: 10.1128/JVI.01039-19, PMID: 31511393
785 Webby, R. J., K. Rossow, G. Erickson, Y. Sims, and R. Webster. 2004. Multiple lineages of
786 antigenically and genetically diverse influenza A virus co-circulate in the United States
787 swine population. *Virus Res* **103**:67-73. DOI: 10.1016/j.virusres.2004.02.015, PMID:
788 15163491
789 Webster, R. G., W. J. Bean, O. T. Gorman, T. M. Chambers, and Y. Kawaoka. 1992. Evolution
790 and ecology of influenza A viruses. *Microbiol Rev* **56**:152-79. DOI:
791 10.1128/mr.56.1.152-179.1992, PMID: 1579108
792 Webster, R. G., and E. A. Govorkova. 2014. Continuing challenges in influenza. *Ann N Y Acad*
793 *Sci* **1323**:115-39. DOI: 10.1111/nyas.12462, PMID: 24891213
794 WHO. 2016. Tool for Influenza Pandemic Risk Assessment (TIPRA). Available at:
795 https://www.who.int/influenza/publications/TIPRA_manual_v1/en/.
796 WHO. 2018. Antigenic and genetic characteristics of zoonotic influenza viruses and candidate
797 vaccine viruses developed for potential use in human vaccines. Available at:
798 https://www.who.int/influenza/vaccines/virus/characteristics_virus_vaccines/en/.
799 Xiao, C., W. Ma, N. Sun, L. Huang, Y. Li, Z. Zeng, Y. Wen, Z. Zhang, H. Li, Q. Li, Y. Yu, Y.
800 Zheng, S. Liu, P. Hu, X. Zhang, Z. Ning, W. Qi, and M. Liao. 2016. PB2-588 V

801 promotes the mammalian adaptation of H10N8, H7N9 and H9N2 avian influenza viruses.
802 *Sci Rep* **6**:19474. DOI: 10.1038/srep19474, PMID: 26782141
803 Yen, H. L., C. H. Liang, C. Y. Wu, H. L. Forrest, A. Ferguson, K. T. Choy, J. Jones, D. D.
804 Wong, P. P. Cheung, C. H. Hsu, O. T. Li, K. M. Yuen, R. W. Chan, L. L. Poon, M. C.
805 Chan, J. M. Nicholls, S. Krauss, C. H. Wong, Y. Guan, R. G. Webster, R. J. Webby, and
806 M. Peiris. 2011. Hemagglutinin-neuraminidase balance confers respiratory-droplet
807 transmissibility of the pandemic H1N1 influenza virus in ferrets. *Proc Natl Acad Sci U S*
808 *A* **108**:14264-9. DOI: 10.1073/pnas.1111000108, PMID: 21825167
809 Zanin, M., S. Duan, S. S. Wong, G. Kumar, P. Baviskar, E. Collin, C. Russell, S. Barman, B.
810 Hause, and R. Webby. 2017. An Amino Acid in the Stalk Domain of N1 Neuraminidase
811 Is Critical for Enzymatic Activity. *J Virol* **91**. DOI: 10.1128/JVI.00868-16, PMID:
812 27847354
813 Zanin, M., B. Marathe, S. S. Wong, S. W. Yoon, E. Collin, C. Oshansky, J. Jones, B. Hause, and
814 R. Webby. 2015. Pandemic Swine H1N1 Influenza Viruses with Almost Undetectable
815 Neuraminidase Activity Are Not Transmitted via Aerosols in Ferrets and Are Inhibited
816 by Human Mucus but Not Swine Mucus. *J Virol* **89**:5935-48. DOI: 10.1128/JVI.02537-
817 14, PMID: 25810540
818 Zaraket, H., T. Baranovich, B. S. Kaplan, R. Carter, M. S. Song, J. C. Paulson, J. E. Rehg, J.
819 Bahl, J. C. Crumpton, J. Seiler, M. Edmonson, G. Wu, E. Karlsson, T. Fabrizio, H. C.
820 Zhu, Y. Guan, M. Husain, S. Schultz-Cherry, S. Krauss, R. McBride, R. G. Webster, E.
821 A. Govorkova, J. H. Zhang, C. J. Russell, and R. J. Webby. 2015. Mammalian adaptation
822 of influenza A(H7N9) virus is limited by a narrow genetic bottleneck. *Nature*
823 *Communications* **6**. DOI: ARTN 6553
824 10.1038/ncomms7553, PMID: WOS:000353693700001

825 Zaraket, H., O. A. Bridges, S. Duan, T. Baranovich, S. W. Yoon, M. L. Reed, R. Salomon, R. J.
826 Webby, R. G. Webster, and C. J. Russell. 2013a. Increased acid stability of the
827 hemagglutinin protein enhances H5N1 influenza virus growth in the upper respiratory
828 tract but is insufficient for transmission in ferrets. *J Virol* **87**:9911-22. DOI:
829 10.1128/JVI.01175-13, PMID: 23824818
830 Zaraket, H., O. A. Bridges, and C. J. Russell. 2013b. The pH of activation of the hemagglutinin
831 protein regulates H5N1 influenza virus replication and pathogenesis in mice. *J Virol*
832 **87**:4826-34. DOI: 10.1128/JVI.03110-12, PMID: 23449784
833 Zhong, L., X. Wang, Q. Li, D. Liu, H. Chen, M. Zhao, X. Gu, L. He, X. Liu, M. Gu, D. Peng,
834 and X. Liu. 2014. Molecular mechanism of the airborne transmissibility of H9N2 avian
835 influenza A viruses in chickens. *J Virol* **88**:9568-78. DOI: 10.1128/JVI.00943-14, PMID:
836 24920791
837

838 **Figures and Figure Legends**

839

840 **Figure 1. Virus characterization *in vitro*.** (A) Sequence variations. Whole genomes of gamma
841 viruses G15-HA1-S210, G15-HA1-N210, G15-HA1-mixed, and P4-PA-mixed were obtained by
842 next-generation sequencing. Amino-acid variations with frequencies ≥ 5% and reads ≥ 10 are
843 shown in colored pie charts. H3 numbering was used for the HA protein. (B) HA activation pH
844 values measured by syncytium assay. Viruses were inoculated into Vero cells at an MOI of 3
845 PFU/cell. Representative images are shown with the HA activation pH in bold. (C) Virus
846 inactivation pH values. Viruses were treated with pH-adjusted PBS, re-neutralized, and subjected
847 to measurement of residual virus infectivity by $TCID_{50}$. (D) Virus growth in MDCK cells. Viruses
848 were inoculated into MDCK cells at an MOI of 2 PFU/cell. Cell-free culture supernatants were
849 harvested at 6- and 8-hours post-infection (hpi) and titrated by $TCID_{50}$. All experiments were
850 independently performed at least twice. *P* values were determined according to one-way ANOVA
851 followed by a Tukey's multiple comparisons test.

852

853 **Figure 2. *In vitro* transcription and replication of G15-HA1-S210 and P4-PA-mixed.** (A)
854 Virus mRNA, cRNA, and vRNA accumulation after 4 hpi. (B) Virus mRNA, cRNA, and vRNA
855 accumulation after 6 hpi. (C) Virus copies released into culture media. G15-HA1-S210 and P4-
856 PA-mixed viruses were inoculated into MDCK cells at an MOI of 2 PFU/cell. At 4 and 6 hpi, the
857 infected MDCK cells were lysed and harvested for total viral RNA. Virus specific mRNA, cRNA,
858 and vRNA were quantified by two-step real-time reverse-transcription PCR using specific primers
859 and normalized to GAPDH mRNA levels. Meanwhile, culture supernatants were harvested for
860 quantification of virions released. Virions released from the cells were quantified by real-time

861 quantitative PCR using plasmid PHW2000-NP (G15-HA1-mixed) as a standard. Virus copies were
862 quantified. *P* values were determined according to Welch's *t* test.
863
864 **Figure 3. Infection of G15-HA1-S210, P4-PA-mixed, and G15-HA1-mixed in inoculated**
865 **donor ferrets.** (A) Viral properties. Relative polymerase activity and HA stability for viruses are
866 shown. (B) Ferret experimental caging. Viruses were intranasally inoculated into 3 donor ferrets
867 per group on day 0. After one day, 3 naïve ferrets were introduced into the same cages and 3 into
868 the adjacent cages. These ferrets were designated contact and airborne ferrets, respectively. Overall,
869 there were 9 ferrets for each cubicle. Each virus had 2 cubicles for a total of 6 donors, 6 contacts,
870 and 6 airborne. (C) $TCID_{50}$ titers of virus in nasal washes from donor ferrets. Ferret nasal washes
871 were collected every other day until day 14. Each bar represents the virus titer of an individual
872 sample, and the dashed lines represent the limit of detection. (D) Day of virus peak titer in donor
873 ferrets. Each symbol represents the day that virus peak titer was observed in an individual donor
874 ferret. (E) Virus peak titers in donor ferrets. Each symbol represents the virus peak titer in an
875 individual donor ferret. (F) Percent body weight of donor ferrets. Ferret body weight was
876 monitored daily until day 14. *P* values were calculated using One-way ANOVA with Turkey's
877 multiple comparisons test.
878
879 The following figure supplements are available for figure 3:
880 **Figure 3-figure supplement 1. Cubicle temperature and relative humidity during ferret**
881 **transmission study.** The ferret experiment was carried out as described in Figure 3A. In each
882 cubicle, temperature (A) and relative humidity (B) were monitored daily until day 14.
883

884 **Figure 3-figure supplement 2. Body temperature changes of donor ferrets.** The ferret
885 experiment was carried out as illustrated in Figure 3A. Body temperatures of donor ferret
886 inoculated with G15-HA1-S210 (A), P4-PA-mixed (B), and G15-HA1-mixed (C) were monitored
887 daily until day 14.
888
889 **Figure 4. Transmission, seroconversion, and the number of viruses isolated in ferrets.** The
890 ferret experiment was carried out as described in Figure 3A. (A) Virus $TCID_{50}$ titers of nasal
891 washes from contact ferrets. (B) Virus $TCID_{50}$ titers of nasal washes from airborne ferrets. (C)
892 HAI titers of day-21 sera of donor, contact, and airborne ferrets. (D) The number of virus isolates
893 from ferret nasal washes of donor, contact, and airborne ferrets.
894
895 The following figure supplements are available for figure 4:
896 **Figure 4-figure supplement 1. Body weight changes of contact and airborne ferrets exposed**
897 **with G15-HA1-S210, P4-PA-mixed and G15-HA1-mixed.** The ferret experiment was carried
898 out as described in Figure 3A. Body weight changes of contact (A) and airborne (B) ferrets were
899 monitored daily until day 14.
900
901 **Figure 4-figure supplement 2. Body temperatures of contact and airborne ferrets exposed**
902 **with G15-HA1-S210, P4-PA-mixed and G15-HA1-mixed**. The ferret experiment was carried
903 out as described in Figure 3A. Body temperatures of contact (A) and airborne (B) ferrets were
904 monitored daily until day 14.
905
906 **Figure 5. Frequencies of single-nucleotide variants (SNVs) for nasal washes collected from**
907 **donor, contact, and airborne ferrets**. The ferret experiment was carried out as described in

908 Figure 3A. The whole-genomes of nasal washes collected from donor, contact, and airborne ferrets
909 infected or exposed with G15-HA1-S210 (A), P4-PA-mixed (B), and G15-HA1-mixed (C) were
910 obtained by next-generation sequencing. SNVs with frequencies ≥ 5% and reads ≥ 10 were read
911 out. Variant PA-S321 in cubicle 2 included reads ≥2 because of poor coverage at PA-321 for these
912 samples. The listed SNVs met the following criteria: (1) resulted in protein sequence changes, and
913 (2) appeared in nasal washes in each cubicle ≥ 2 times and/or frequencies greater than 30%. The
914 frequencies of SNVs are represented by the colored boxes. Each column represents the SNVs for
915 one ferret nasal wash.
916
917 **Figure 6. The proportions of minor variant PA-S321 and correlation with polymerase**
918 **activity.** (A) The proportions of PA-S321 in P4-PA-mixed from the original inoculum and
919 infected/exposed ferrets. (B) Evaluation of polymerase activity of P4-PA-S321. The experiment
920 was performed as described in Figure 2. The transcription and replication of virus containing 100%
921 variant PA-S321 were compared to those of G15-HA1-S210 and P4-PA-mixed. The experiments
922 were independently performed twice. *P* values were determined according to one-way ANOVA
923 followed by a Tukey's multiple comparisons test.
924
925 **Figure 7. The proportions of minor variant HA1-S210 and correlation with HA stability.** (A)
926 The proportions of HA1- S210 in G15-HA1-mixed from the original inoculum and
927 infected/exposed ferrets. (B-D) Virus HA activation pH values of isolates from G15-HA1-mixed,
928 G15-HA1-S210, and P4-PA-mixed infected/exposed ferrets. Virus isolates from nasal washes
929 were propagated in MDCK cells once. Syncytium assay were performed to measure the HA
930 activation pH values of these isolates.
931

932 **Figure 8. Relative polymerase activities and HA stabilities in ferrets.** Relative polymerase

933 activity and HA activation pH were compared for inoculated virus (left) and after airborne

934 transmission in ferrets (right). Each symbol represents an individual ferret.

935

936 **Table 1. Virus characteristics before and after infection and transmission in ferrets.**

Virus characterization		G15-HA1-S210	P4-PA-mixed	G15-mixed	G15-HA1-N210
Genotype variations	HA1-210	S	S	85% N, 15% S	N
	PB2-648	L	M	L	L
	PA-271	P	T	P	P
	PA-321	N	92% N, 8%S	N	N
	PA-386	D	86% D, 14% N	D	D
Phenotype variations *in vitro*	HA activation pH [a]	5.6	5.5	5.8	5.8
	HA inactivation pH [b]	5.6	5.6	5.75	5.8
	Polymerase activity	higher	lower	higher	higher
	One-step growth	higher	lower	higher	highest
Donor ferrets	Virus growth (log_{10} $TCID_{50}$)	7.3 (± 0.67)	5.8 (± 1)	5.0 (± 0.28)	- [f]
	Number of isolates from ferrets [c]	9; 9	9; 9	9; 9	-
	Seroconversion [d]	3/3; 3/3	3/3; 3/3	3/3; 3/3	-
	Day of peak titers	1	2.7 (± 1.5)	3	-
	Peak titers (log_{10} $TCID_{50}$)	7.3 (± 0.67)	6.7 (± 0.43)	6.2 (± 0.54)	-
	Major variants	none	PA-S321	HA1-S210	-
	HA activation pH range	5.5-5.6	5.5-5.6	5.5-5.9	-
Contact ferrets	Number of isolates from ferrets	9; 10	9; 10	9; 10	-
	Seroconversion	3/3; 3/3	3/3; 3/3	3/3; 3/3	-
	HA activation pH range	5.5-5.6	5.5-5.6	5.6-5.9	-
	Major variants	none	PA-S321	HA1-S210	-
Airborne ferrets	Number of isolates from ferrets	7; 3	4; 2	3; 0	-
	Days for virus shedding	8-14; 2-6	8-14; 10-14	-; 8-12	-
	Seroconversion	3/3; 1/3	3/3; 1/3	2/3; 3/3	-
	Major variants	sporadic	PA-S321	HA1-S210	-
	Polymerase activity	higher	higher & lower	higher	-
	HA activation pH [e]	5.5-5.6	5.5-5.6	~5.6	-

937 [a] HA activation pH measured by syncytia assay.

938 [b] HA inactivation pH measured by treating viruses with indicated pH and titrating resulting virions by $TCID_{50}$.

939 [c] The Number of isolates is listed for those grown successfully in MDCK cells after recovery from ferrets in cubicle

940 1 and cubicle 2.

941 [d] Data for each virus is listed for each cubicle with the first X/Y number representing cubicle 1 and the second X/Y

942 representing cubicle 2.

943 [e] HA activation pH of airborne-transmitted virus on first day of isolation.

944 [f] -, Not measured.

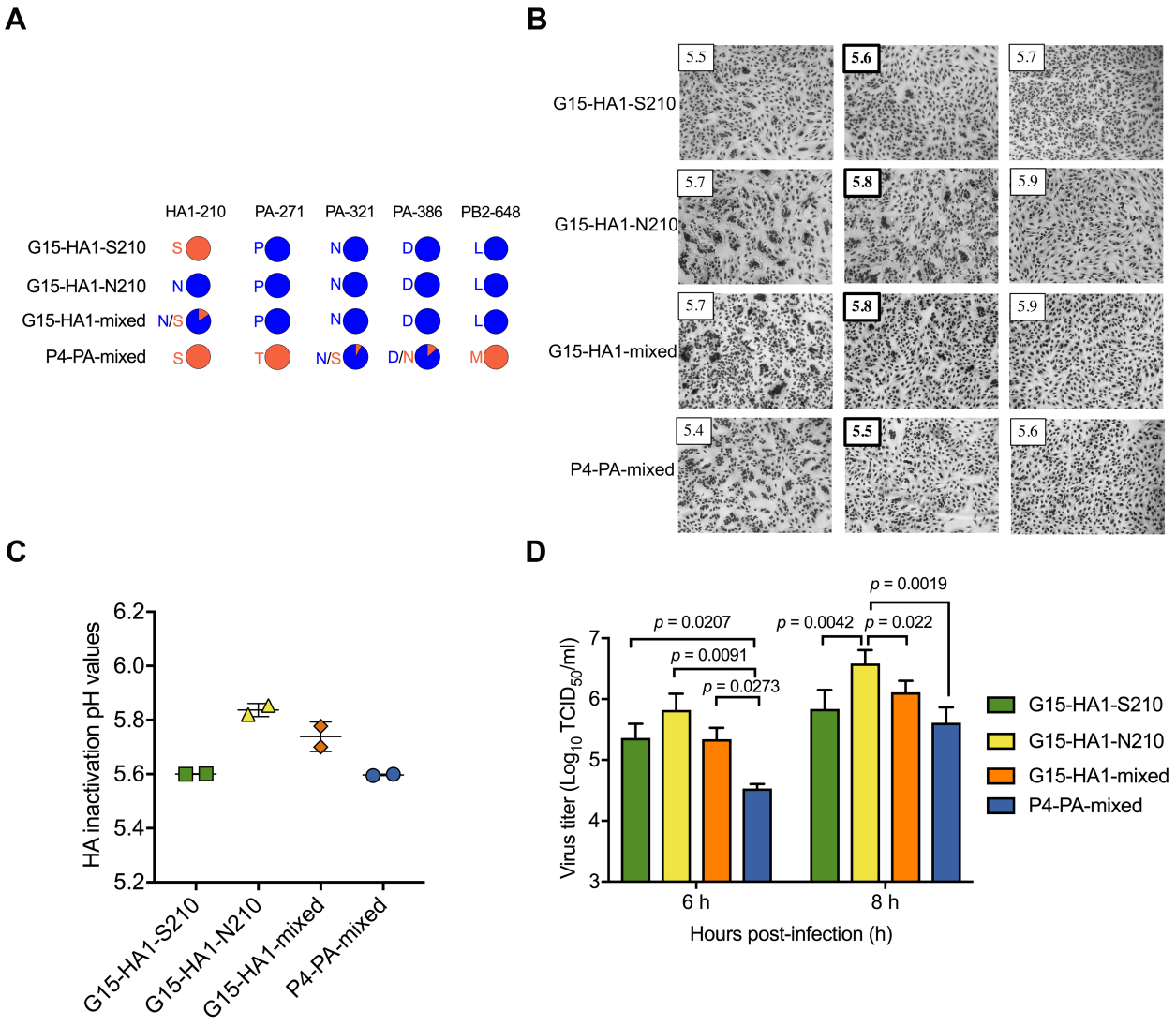
A
HA1-210
PA-271
PA-321
PA-386
PB2-648
G15-HA1-S210
G15-HA1-N210
G15-HA1-mixed
P4-PA-mixed
S
P
N
D
L
N
P
N
D
L
N/S
P
N
D
L
S
T
N/S
D/N
M
B
G15-HA1-S210
G15-HA1-N210
G15-HA1-mixed
P4-PA-mixed
5.5
5.6
5.7
5.7
5.8
5.9
5.7
5.8
5.9
5.4
5.5
5.6
C
HA inactivation pH values
6.2
6.0
5.8
5.6
5.4
5.2
G15-HA1-S210
G15-HA1-N210
G15-HA1-mixed
P4-PA-mixed
D
Virus titer (Log10 TCID50/ml)
7
6
5
4
3
p = 0.0207
p = 0.0091
p = 0.0273
p = 0.0042
p = 0.022
p = 0.0019
6 h
8 h
Hours post-infection (h)
G15-HA1-S210
G15-HA1-N210
G15-HA1-mixed
P4-PA-mixed

Figure 1

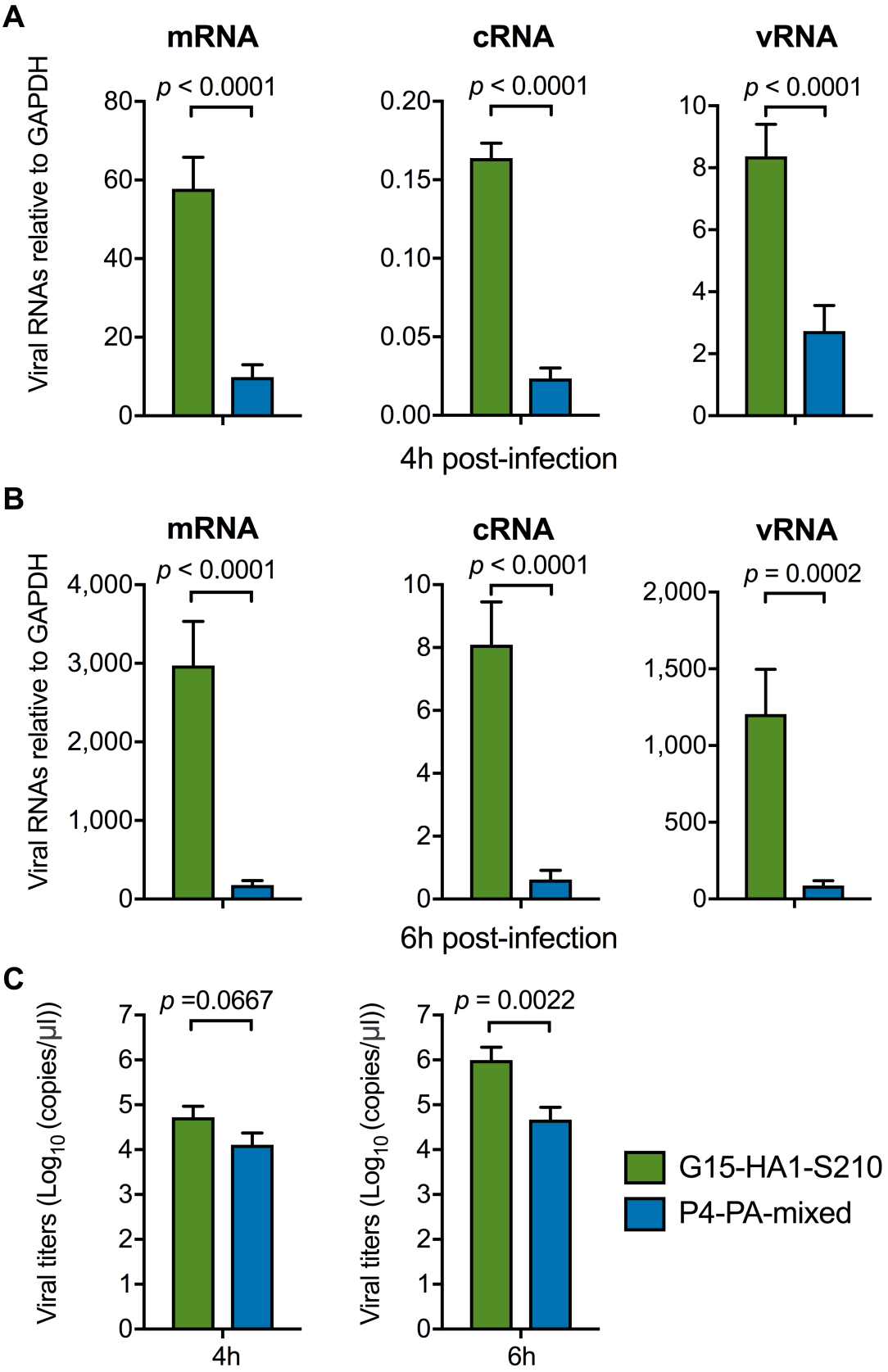
A
mRNA
cRNA
vRNA
Viral RNAs relative to GAPDH
p < 0.0001
p < 0.0001
p < 0.0001
4h post-infection
B
mRNA
cRNA
vRNA
Viral RNAs relative to GAPDH
p < 0.0001
p < 0.0001
p = 0.0002
6h post-infection
C
Viral titers (Log10 (copies/µl))
p =0.0667
p = 0.0022
4h
6h
G15-HA1-S210
P4-PA-mixed

Figure 2

A

	Relative polymerase activity	HA activation pH
G15-HA1-S210	Higher	5.6
P4-PA-mixed	Lower	5.5
G15-HA1-mixed	Higher	5.8

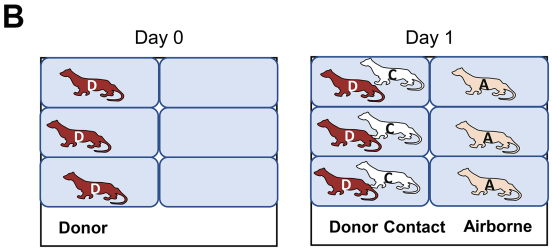

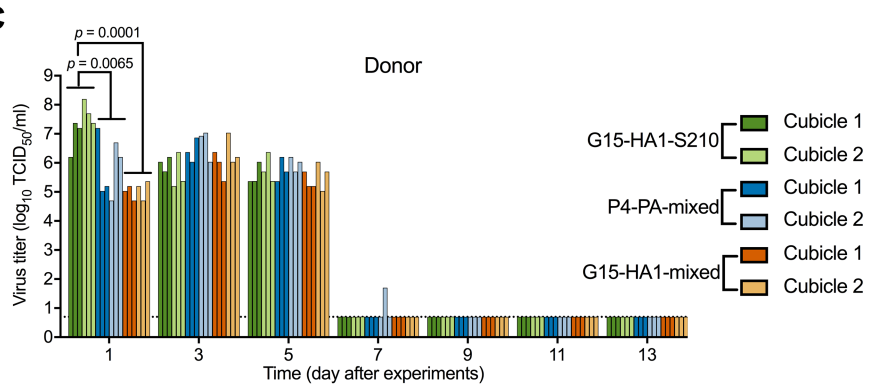

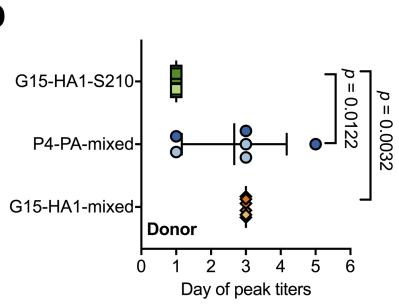

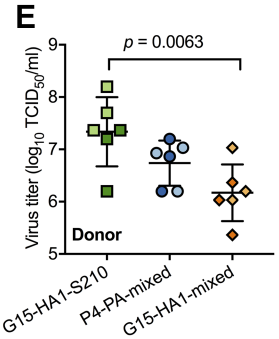

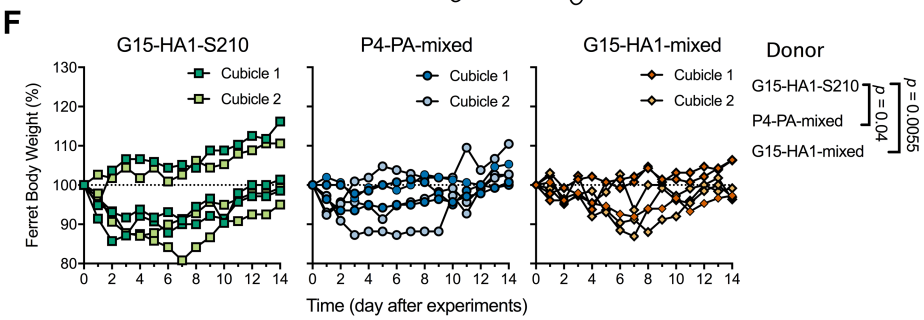

Figure 3

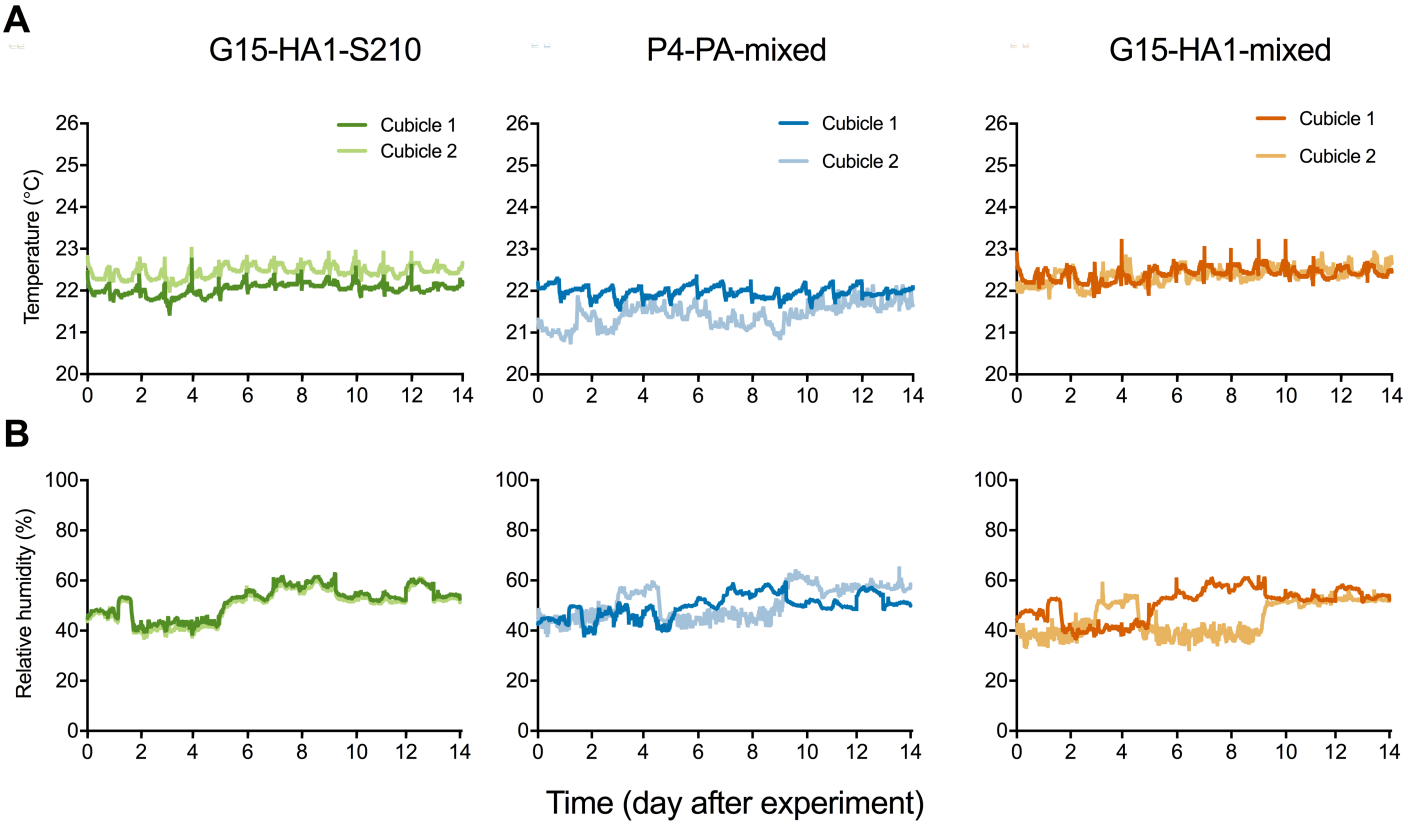

Figure 3-figure supplement 1

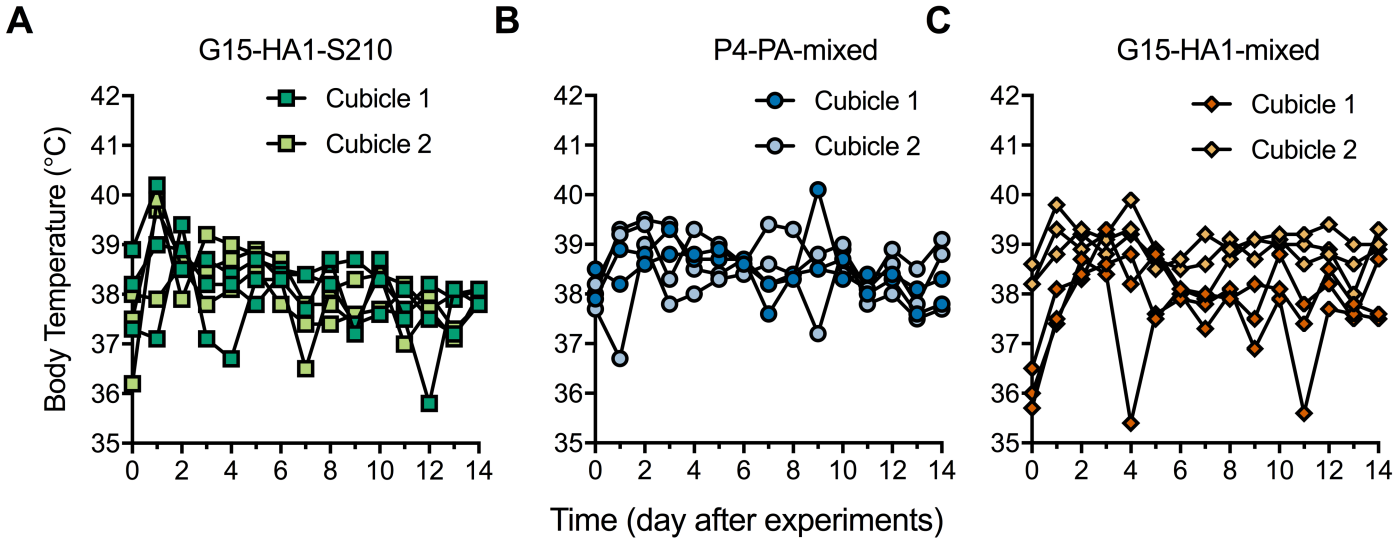

Figure 3-figure supplement 2

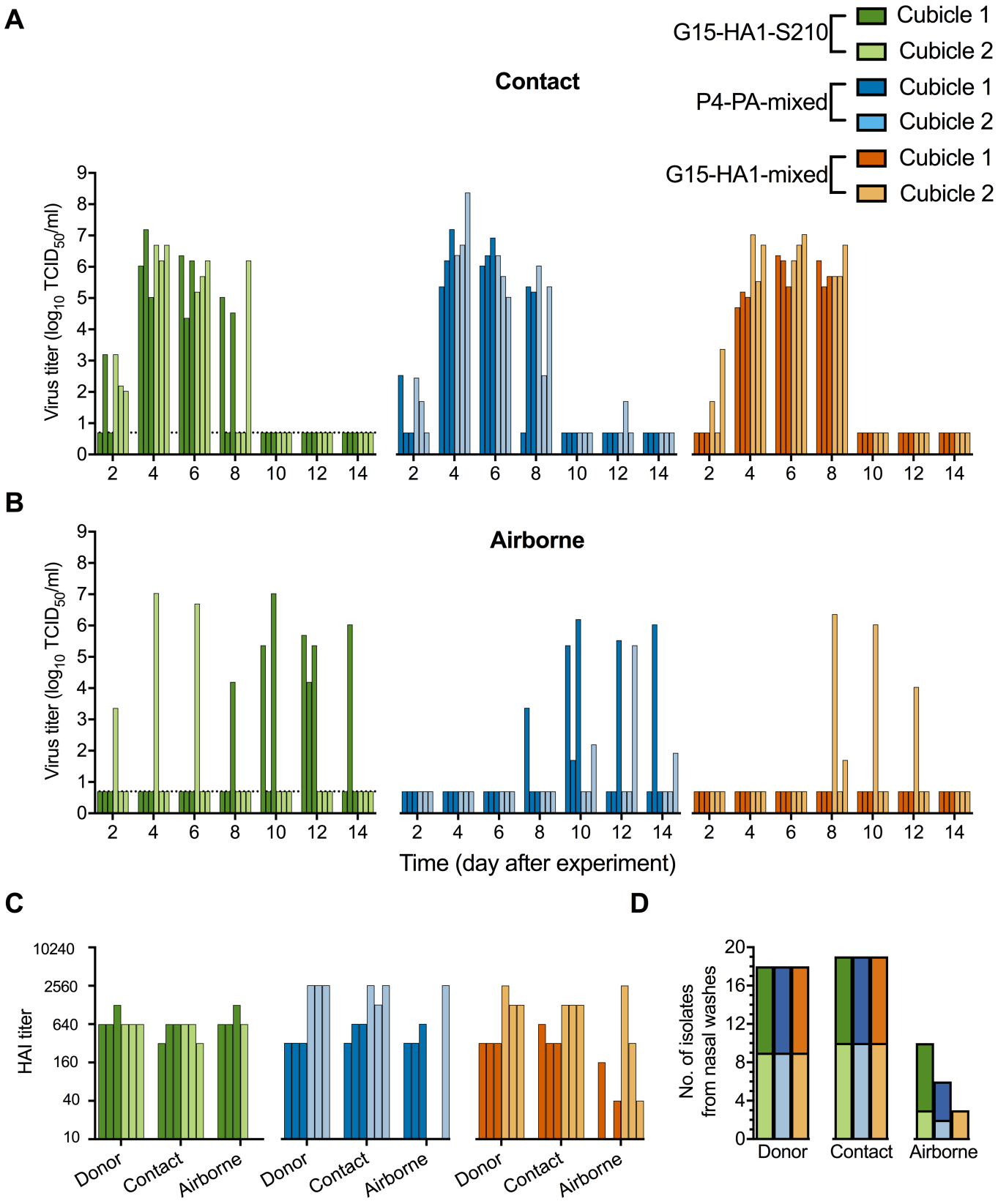
A
Contact
G15-HA1-S210
Cubicle 1
Cubicle 2
P4-PA-mixed
Cubicle 1
Cubicle 2
G15-HA1-mixed
Cubicle 1
Cubicle 2
Virus titer (log10 TCID50/ml)
B
Airborne
Virus titer (log10 TCID50/ml)
Time (day after experiment)
C
HAI titer
10240
2560
640
160
40
10
Donor
Contact
Airborne
D
No. of isolates from nasal washes
Donor
Contact
Airborne

Figure 4

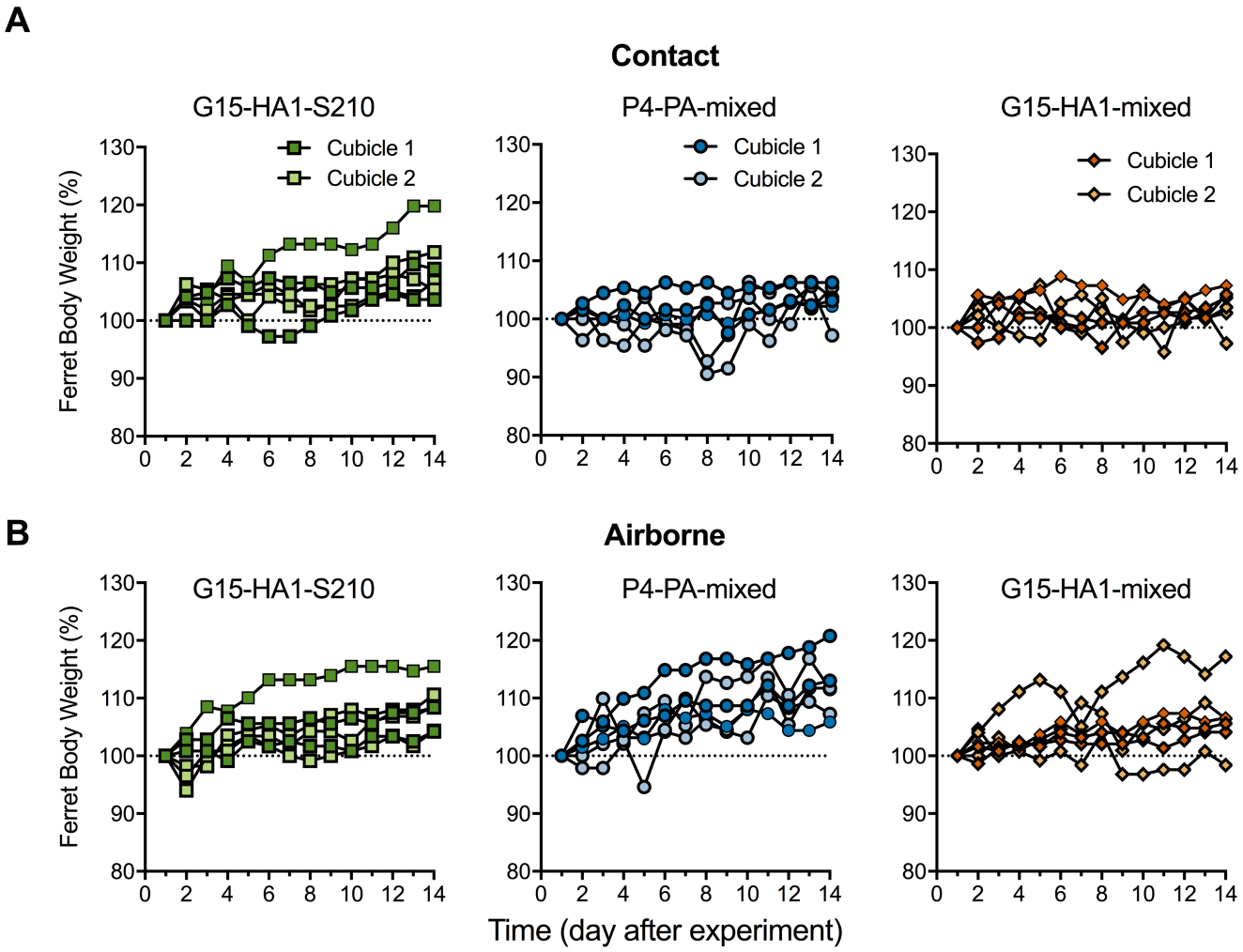

Figure 4-figure supplement 1

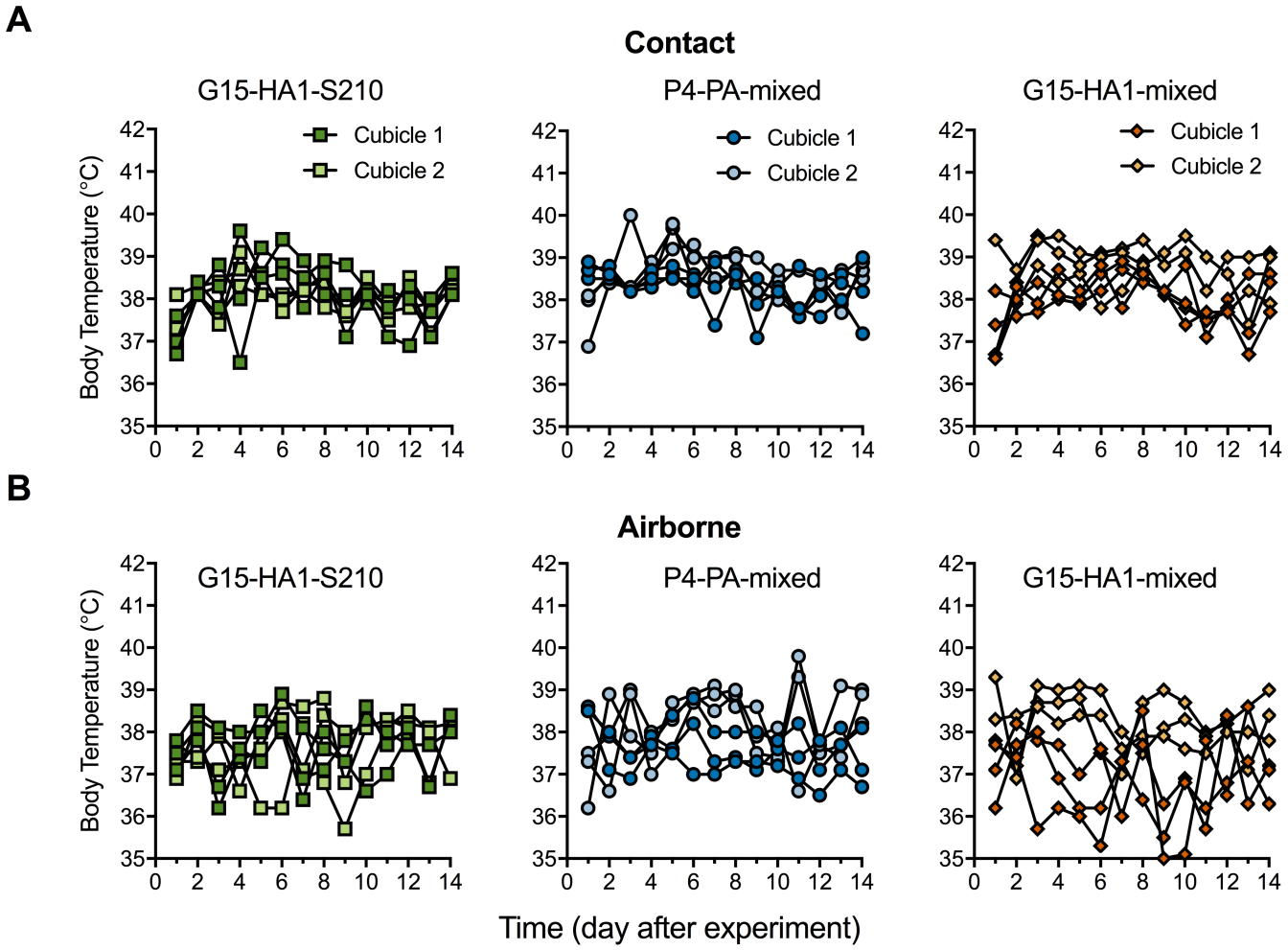

Figure 4-figure supplement 2

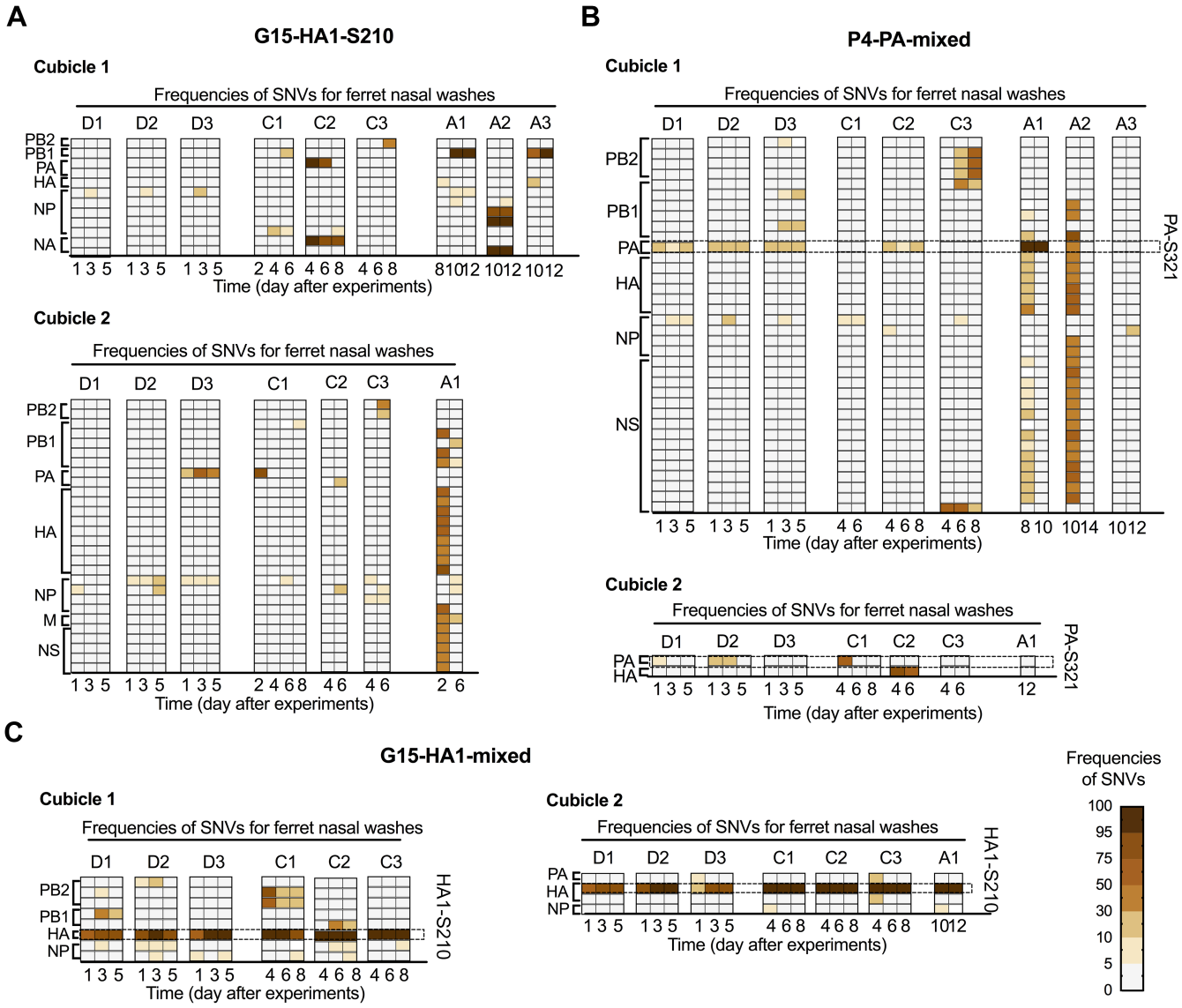
A
G15-HA1-S210
Cubicle 1
Frequencies of SNVs for ferret nasal washes
D1 D2 D3 C1 C2 C3 A1 A2 A3
PB2
PB1
PA
HA
NP
NA
1 3 5 1 3 5 1 3 5 2 4 6 4 6 8 4 6 8 8 10 12 10 12 10 12
Time (day after experiments)
Cubicle 2
Frequencies of SNVs for ferret nasal washes
D1 D2 D3 C1 C2 C3 A1
PB2
PB1
PA
HA
NP
M
NS
1 3 5 1 3 5 1 3 5 2 4 6 8 4 6 4 6 2 6
Time (day after experiments)
B
P4-PA-mixed
Cubicle 1
Frequencies of SNVs for ferret nasal washes
D1 D2 D3 C1 C2 C3 A1 A2 A3
PB2
PB1
PA
HA
NP
NS
PA-S321
1 3 5 1 3 5 1 3 5 4 6 4 6 8 4 6 8 8 10 10 14 10 12
Time (day after experiments)
Cubicle 2
Frequencies of SNVs for ferret nasal washes
D1 D2 D3 C1 C2 C3 A1
PA
HA
PA-S321
1 3 5 1 3 5 1 3 5 4 6 8 4 6 4 6 12
Time (day after experiments)
C
G15-HA1-mixed
Cubicle 1
Frequencies of SNVs for ferret nasal washes
D1 D2 D3 C1 C2 C3
PB2
PB1
HA
NP
HA1-S210
1 3 5 1 3 5 1 3 5 4 6 8 4 6 8 4 6 8
Time (day after experiments)
Cubicle 2
Frequencies of SNVs for ferret nasal washes
D1 D2 D3 C1 C2 C3 A1
PA
HA
NP
HA1-S210
1 3 5 1 3 5 1 3 5 4 6 8 4 6 8 4 6 8 10 12
Time (day after experiments)
Frequencies of SNVs
100
95
75
50
30
10
5
0

Figure 5

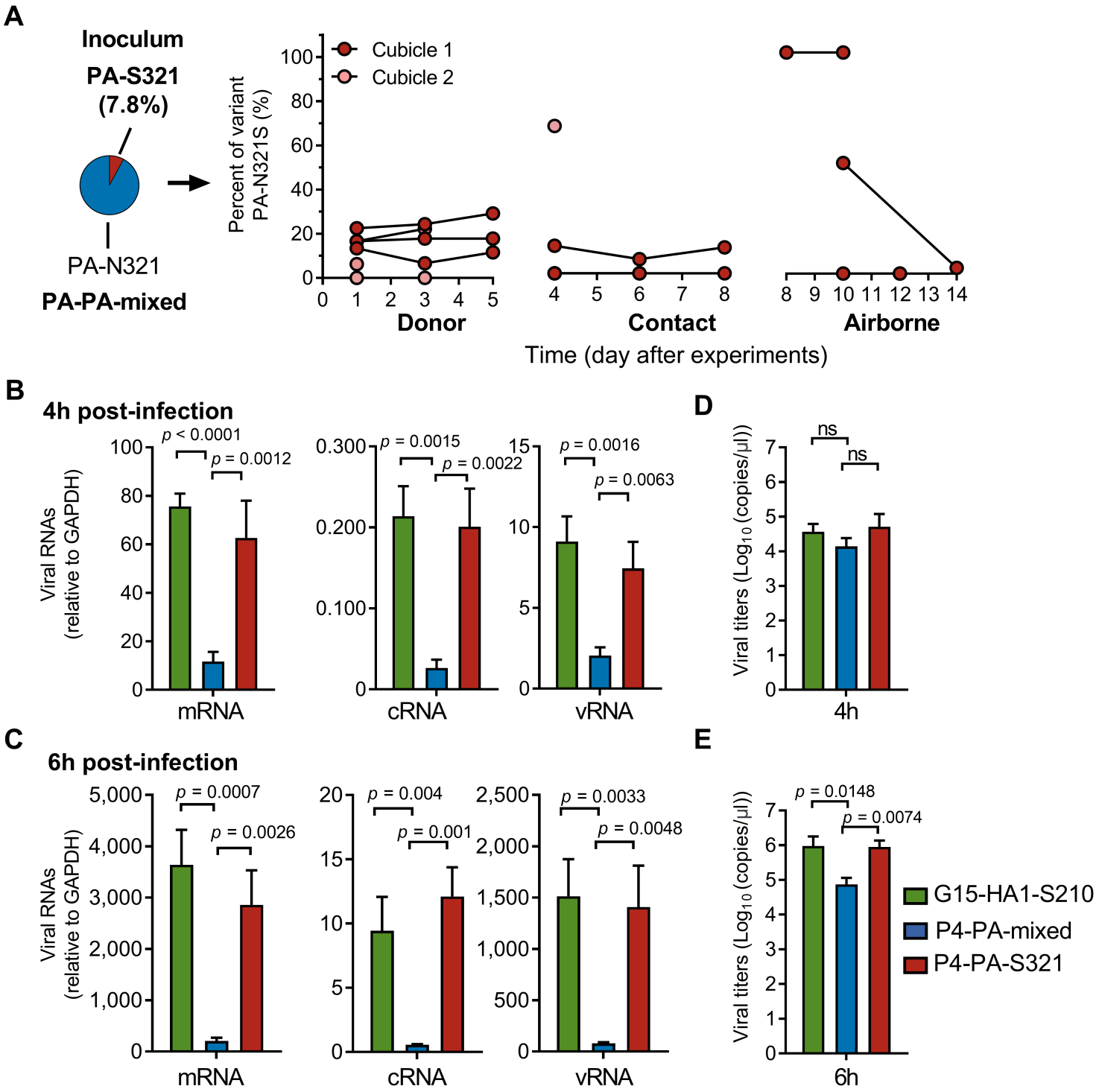
A
Inoculum
PA-S321
(7.8%)
PA-N321
PA-PA-mixed
Cubicle 1
Cubicle 2
Percent of variant
PA-N321S (%)
Donor
Contact
Airborne
Time (day after experiments)
B
4h post-infection
Viral RNAs
(relative to GAPDH)
p < 0.0001
p = 0.0012
p = 0.0015
p = 0.0022
p = 0.0016
p = 0.0063
mRNA
cRNA
vRNA
C
6h post-infection
p = 0.0007
p = 0.0026
p = 0.004
p = 0.001
p = 0.0033
p = 0.0048
D
Viral titers (Log10 (copies/µl))
ns
ns
4h
E
p = 0.0148
p = 0.0074
6h
G15-HA1-S210
P4-PA-mixed
P4-PA-S321

Figure 6

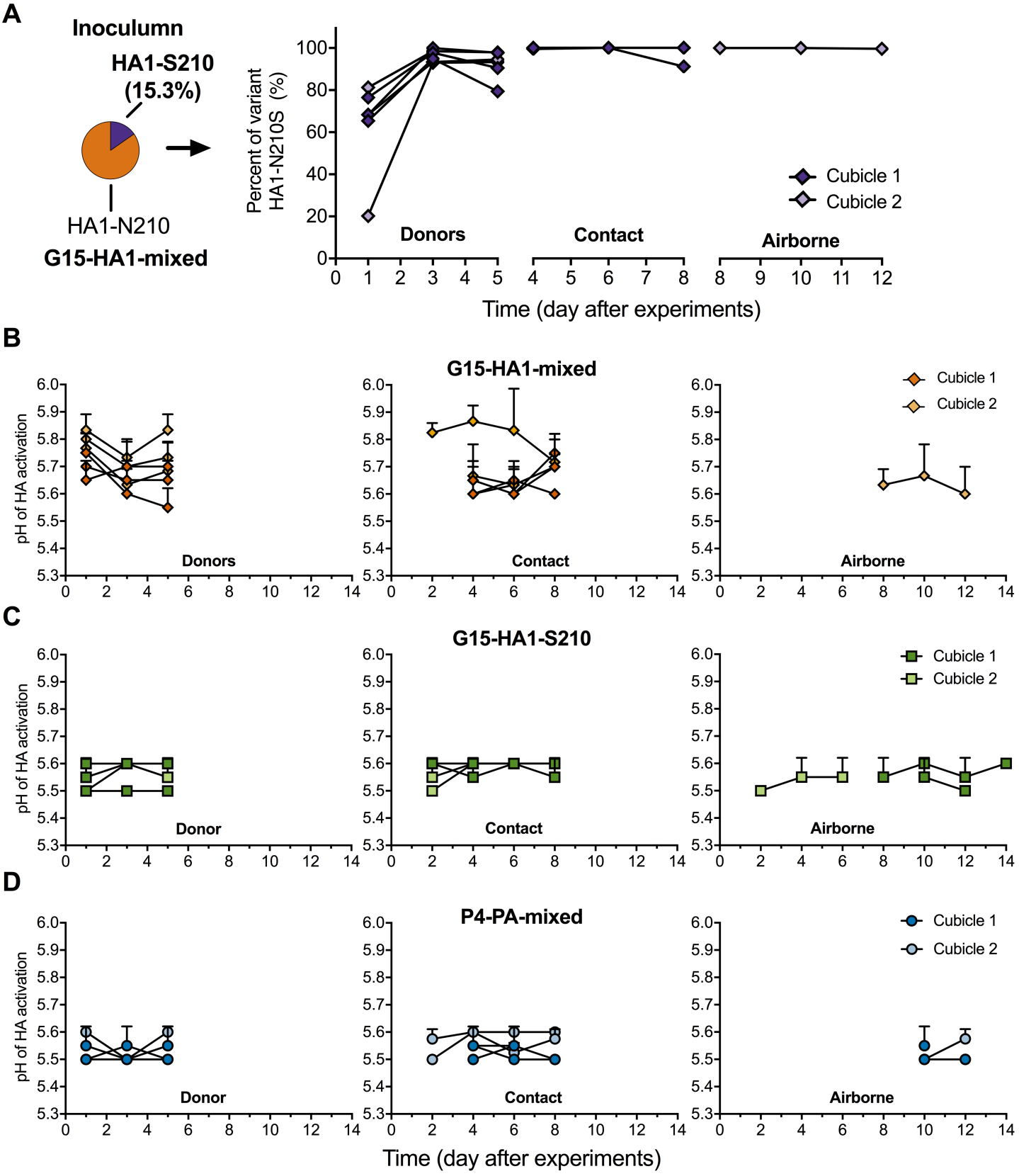
A
Inoculumn
HA1-S210
(15.3%)
HA1-N210
G15-HA1-mixed
Percent of variant HA1-N210S (%)
Donors
Contact
Airborne
Cubicle 1
Cubicle 2
Time (day after experiments)
B
G15-HA1-mixed
pH of HA activation
Donors
Contact
Airborne
Cubicle 1
Cubicle 2
C
G15-HA1-S210
Donor
Contact
Airborne
D
P4-PA-mixed
Donor
Contact
Airborne
Time (day after experiments)

Figure 7

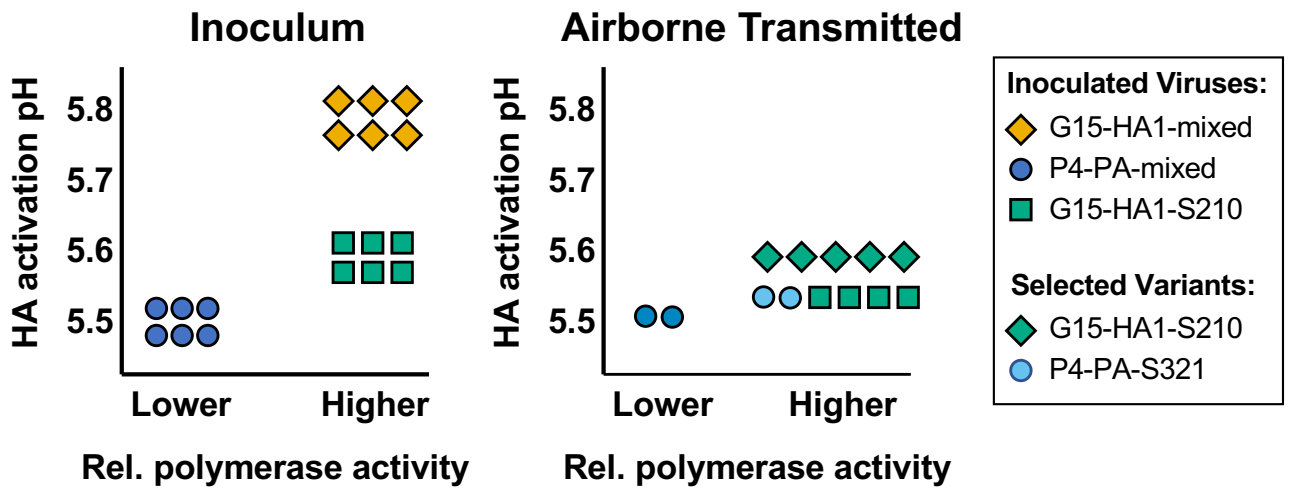
Inoculum
Airborne Transmitted
HA activation pH
5.8
5.7
5.6
5.5
Lower
Higher
Rel. polymerase activity
Inoculated Viruses:
G15-HA1-mixed
P4-PA-mixed
G15-HA1-S210
Selected Variants:
G15-HA1-S210
P4-PA-S321

Figure 8